FINITE TYPE INVARIANTS OF W-KNOTTED OBJECTS III: W-FOAMS, THE KASHIWARA-VERGNE THEOREM AND DRINFEL'D ASSOCIATORS

DROR BAR-NATAN AND ZSUZSANNA DANCSO

Abstract. This is the third in a series of papers studying the finite type invariants of various w-knotted objects and their relationship to the Kashiwara-Vergne problem and Drinfel'd associators. In this paper we present a topological solution to the Kashiwara-Vergne problem. In particular we recover via a topological argument the Alkeseev-Enriquez-Torossian [AET] formula for explicit solutions of the Kashiwara-Vergne equations in terms of associators.

We study a class of w-knotted objects: knottings of *2-dimensional foams* and various associated features in four-dimensioanl space. We use a topological construction which we name the double tree construction to show that every *expansion* (also known as *universal finite type invariant*) of parenthesized braids extends first to an expansion of knotted trivalent graphs (a well known result), and then extends uniquely to an expansion of the w-knotted objects mentioned above.

In algebraic language, an expansion for parenthesized braids is uniquely determined by *Drinfel'd associator* Φ, and an expansion for w-knotted objects is uniquely determined by a solution V of the Kashiwara-Vergne problem [KV], as reformulated by Alekseev and Torossian [AT]. Hence our result provides a topological framework for the result of [AET] that "there is a formula for V in terms of Φ", along with an independent topological proof of the Kashiwara-Vergne Theorem and the Alekseev-Enriquez-Torossian formula.

Contents

Date: first edition in future, this edition Nov. 15, 2022. The arXiv:????.???? edition may be older.

1991 *Mathematics Subject Classification.* 57M25.

Key words and phrases. virtual knots, w-braids, w-knots, w-tangles, knotted graphs, finite type invariants, Kashiwara-Vergne, associators, double tree, free Lie algebras.

The first author's work was partially supported by NSERC grants RGPIN-264374 and RGPIN-2018-04350, and by the Chu Family Foundation (NYC), and wishes to thank the Sydney Mathematics Research Institute for their hospitality and support. The second author was partially supported by NSF grant no. 0932078 000 while in residence at the Mathematical Sciences Research Institute, and by the Australian Research Council DECRA DE170101128 Fellowship. Electronic version and related files at [WKO3], http://www.math.toronto.edu/~drorbn/papers/WKO3/.

1. Introduction

1.1. **Executive Summary.** This brief section is a large-scale overview of the main result of this paper and the idea behind its proof; it is followed by a detailed introduction.

A *homomorphic expansion* for a class of topological objects $\mathcal{K}$ is an invariant $Z\colon \mathcal{K} \to \mathcal{A}$ whose target space $\mathcal{A}$ is canonically associated with $\mathcal{K}$ (its *associated graded*). Homomorphic expansions satisfy a certain universality property, and respect operations which exist on $\mathcal{K}$ and therefore also on $\mathcal{A}$. Such invariants are often hard to find, and when they are found, they are often intimately connected with deep mathematics, in particular, quantum algebra and Lie theory:

- For many classes of knotted objects in 3-dimensional spaces homomorphic expansions don't exist — for example, one would have loved ordinary tangles to have homomorphic expansions, but they don't.
- Yet a certain class $\mathcal{K}^u$ of knotted objects in 3-space, *parenthesized tangles*, or nearly-equivalently, *knotted trivalent graphs* – which we adopt in this paper and denote by *sKTG* – do have homomorphic expansions. A homomorphic expansion $Z^u\colon \mathcal{K}^u \to \mathcal{A}^u$ is defined by its values on a couple of elements of $\mathcal{K}^u$ which generate $\mathcal{K}^u$ using the operations $\mathcal{K}^u$ is equipped with. The most interesting of these generators is the tetrahedron ⧋, and $\Phi = Z^u(\text{⧋})$ turns out to be equivalent to a *Drinfel'd associator*.
- A certain class $\mathcal{K}^w$ of graphs, called *w-foams* and denoted *wTF*^{o} in the paper – the name is based on a conjectured equivalence to a class of 2-dimensional *welded* knotted tubes in 4-dimensional space – also has homomorphic expansions. The most interesting generator of $\mathcal{K}^w$ is the *vertex* $\curlyvee$, and if $Z^w\colon \mathcal{K}^w \to \mathcal{A}^w$ is a homomorphic expansion, then it turns out that $V = Z^w(\curlyvee)$ is equivalent to a solution of the *Kashiwara-Vergne problem* in Lie theory.

Roughly speaking, $\mathcal{K}^u$ is a part of $\mathcal{K}^w$ and $\mathcal{A}^u$ is a part of $\mathcal{A}^w$, as in the figure on the right (more precisely, there are natural maps $a\colon \mathcal{K}^u \to \mathcal{K}^w$ and $\alpha\colon \mathcal{A}^u \to \mathcal{A}^w$). The main purpose of this paper is to prove the following theorem, whose precise version is stated later as Theorem 1.1:

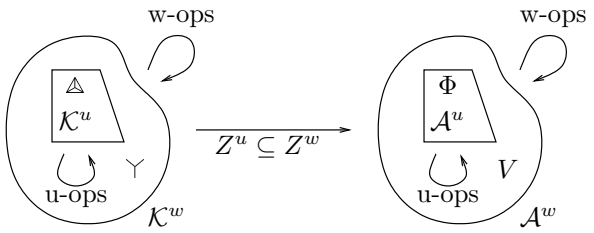

Theorem. Any homomorphic expansion Z^u for $\mathcal{K}^u$ extends uniquely to a homomorphic expansion Z^w for $\mathcal{K}^w$, and therefore, any Drinfel'd associator Φ gives rise to a solution V of the Kashiwara-Vergne problem.

The proof of this theorem is conceptually simple: we show that the generators of $\mathcal{K}^w$ can be explicitly expressed using the generators of $\mathcal{K}^u$ and the operations of $\mathcal{K}^w$, and that the resulting explicit formulas for $Z^w(\curlywedge)$ (and for Z^w of the other generators) satisfies all the required relations.

The devil is in the details. It is in fact impossible to express the generators of $\mathcal{K}^w$ in terms of the generators of $\mathcal{K}^u$ — to do that, one first has to pass to a larger space $\tilde{\mathcal{K}}^w$ (in the paper $\widetilde{wTF}$) that has more objects and more operations, and in which the desired explicit expressions do exist. But even in $\tilde{\mathcal{K}}^w$ these expressions are complicated, and in order to verify the relations they need to be expressed using the framework of a multi-step "double tree construction". A brief pictorial summary of the construction is below, and the explanation takes up the bulk of this paper:

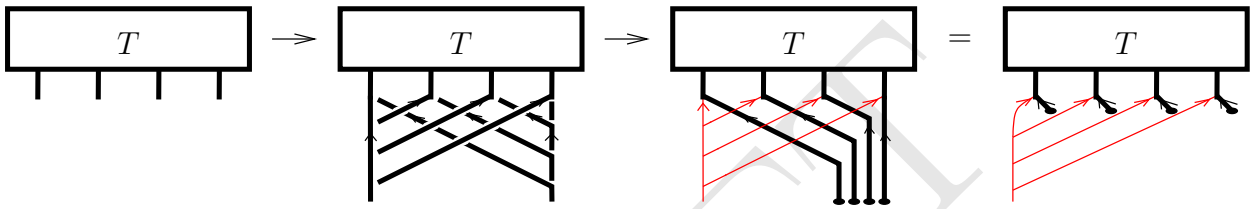

1.2. **Detailed Introduction.** This paper is the third in a sequence [WKO1, WKO2, WKO3] studying finite type invariants of w-knotted objects, and contains the strongest result: a topological construction for a homomorphic expansion of *w-foams* from the Kontsevich integral. This in particular implies the Kashiwara-Vergne Theorem of Lie theory, more precisely, it gives the [AET] formula for solutions of the Kashiwara-Vergne equations in terms of Drinfel'd associators.

The papers in this sequence need not be read consecutively. Readers broadly familiar with finite type invariants will have no trouble reading [WKO2] and this paper without having read [WKO1]. However, the setup and main results of [WKO2] are used heavily in this paper. Reproducing all necessary details would be lengthy, but we include concise summaries for readers already familiar with the content, and otherwise refer to specific results or sections of [WKO2] throughout.

The Kashiwara-Vergne conjecture (KV for short) — proposed in 1978 [KV] and proven in 2006 by Alekseev and Meinrenken [AM] — asserts that solutions exist for a certain set of equations in the space of "tangential automorphisms" of the free lie algebra on two generators. For a precise statement we refer the reader to [WKO2, Section 4.4] or [AT, Section 5.3]. The existence of such solutions has strong implications in Lie theory and harmonic analysis, in particular it implies the multiplicative property of Duflo isomorphism, which was shown to be knot-theoretic in [BLT, BDS].

In [AT] Alekseev and Torossian give another proof of the KV conjecture based on a deep connection with Drinfel'd associators. In turn, Drinfel'd's theory of associators [Dr] can be interpreted as a theory of well-behaved universal finite type invariants of parenthesized tangles[1] [LM, BN2], or of knotted trivalent graphs [Da]. In [AET] Alekseev, Enriquez and Torossian gave an explicit formula for solutions of the Kashiwara-Vergne equations in terms of Drinfel'd associators.

[1] "q-tangles" in [LM], "non-associative tangles" in [BN2].

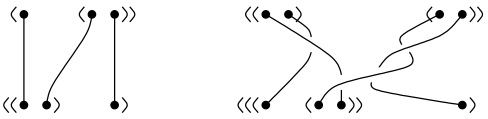

Figure 1. Two examples of parenthesized braids. Note that by convention the parenthetization can be read from the distance scales between the endpoints of the braid, and so we omit the parentheses in parts of this paper.

fig:PBexam

Bar-NatanDancso:WKO2

In [WKO2] we re-interpreted the Kashiwara-Vergne conjecture as the problem of finding a "homomorphic" universal finite type invariant of a class of knotted trivalent tubes in 4-dimansional space (called w-tangled foams), and explained the connection to Drinfel'd associators in terms of a relationship between 3-dimensional and 4-dimensional topology.

Another topological interpretation for the KV problem in terms of the Goldman-Turaev Lie bialgabre later emerged in [AKKN1, AKKN2], and the papers [M] and [AN] contain constructions of Goldman-Turaev expansions from the Kontsevich integral and the Knizhnik-Zamolodchikov connection, respectively.

AKKM:GoldmanTuraev AKKM:GTReverse Massuyeau:TelekseevMaef:GTKZ

In this paper we present a topological construction for a homomorphic universal finite type invariant of w-tangled foams, thereby giving a new topological proof for the KV conjecture. This construction also leads to an explicit formula for KV-solutions in terms of Drinfel'd associators, which we prove agrees with the formula [AET, Theorem 4].

EnriquezTorossian:ExplicitSolutions

Finally, we mention that a *circuit algebra*, which provides the algebraic structure to w-foams, were identified as equivalent to the operadic structure of a *wheeled prop* in [DHR1]. The symmetry groups of Kashiwara-Vergne solutions, called the Kashiwara-Vergne groups, are shown to be automorphism groups of the w-foam circuit algebra and its associated graded arrow diagrams in [DHR2]. The relationship between the symmetries of Drinfel'd associators – the Grothendieck-Teichmuller groups – and the Kashiwara-Vergne groups is described in the topological context of w-foams in the forthcoming paper [DHaR]

DHR:CircAlg DHR:KVARV DHaR:GRTaKV

1.2.1. *Topology.* We begin by describing a chain of maps from "parenthesized braids" to "(signed) knotted trivalent graphs" to "w-tangled foams":

$$\mathcal{K} := \{uPaB \xrightarrow{\text{cl}} sKTG \xrightarrow{a} \widetilde{wTF}\}.$$

Let us first briefly elaborate on each of these spaces and maps.

Parenthesized braids are braids whose ends are ordered along two lines, the "bottom" and the "top", along with parenthetizations of the endpoints on the bottom and on the top. Two examples are shown in Figure 1. Parentehesized braids form a category whose objects are parenthetizations, morphisms are the parenthesized braids themselves, and composition is given by stacking. In addition to stacking, there are several operations defined on parenthesized braids: strand addition, removal and doubling. A detailed introduction to parenthesized braids is in [BN1].

fig:PBexample Bar-Natan:GT1

Trivalent graphs are oriented graphs with three edges meeting at each vertex and whose vertices are equipped with a cyclic orientation of the incident edges. A knotted trivalent graph (KTG) is a framed embedding of a trivalent graph into $\mathbb{R}^3$. KTGs are studied from a finite type invariant point of view in [BND1]. In this paper we use a version of KTGs that was introduced and studied in [WKO2, Section 4.6], namely trivalent tangles with one or two ends and with some extra combinatorial information: trivalent vertices are equipped with a marked "distinguished edge" and signs. We call this space *sKTG* (for signed KTGs), as in [WKO2]. An example is shown on the right. The space *sKTG* is also equipped with several operations: tangle insertion, sticking a 1-tangle onto an edge of another tangle, disjoint union of 1-tangles, edge unzip, and edge orientation switch (see [WKO2, Section 4.6] for details).

The space $\widetilde{wTF}$ is a minor extension of the space wTF^o studied in [WKO2, Section 4.1 – 4.4], and will be introduced in detail in Section 2. It can be described as a circuit algebra (similar to a planar algebra but with non-planar connections allowed, see [WKO2, Section 2.4]) generated by certain features (various kinds of crossings and vertices, as well as "caps") modulo certain relations ("Reidemeister moves") and equipped with a number of auxiliary operations beyond the circuit algebra compositions. This Reidemeister theory conjecturally represents knotted tubes in 4-dimensional space with singular *foam vertices*, caps, and attached one-dimensional strings.

The map cl : $uPaB \to sKTG$ is the "closure map". Given a parenthesized braid, close up its top and bottom each by gluing a binary tree according to the parentetization; this produces a *sKTG* with the convention that all strands are oriented upwards, bottom vertices are negative, and top vertices are positive. An example is shown below.

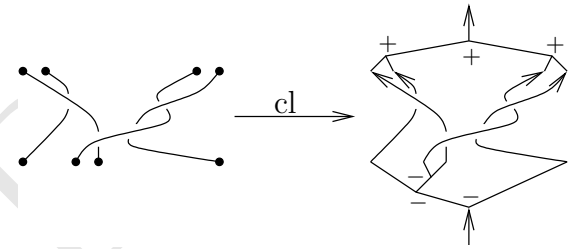

(1) eq:cl

The map $a : sKTG \to \widetilde{wTF}$ arises combinatorially from the fact that all *sKTG* diagrams can be interpreted as elements of $\widetilde{wTF}$, and all $sKTG$ Reidemeister moves are also imposed in $\widetilde{wTF}$. Topologically, it is an extended version of Satoh's tubing map, described in Remark 3.1.1 of [WKO2].

1.2.2. *Algebra.* The chain of maps $\mathcal{K}$ is an example of a general "algebraic structure", as discussed in [WKO2, Section 2.1]. An algebraic structure consists of a collection of objects belonging to a number of "spaces" or "different kinds", and operations that may be unary, binary, multinary or nullary, between these spaces. In this case there are many spaces (or kinds of objects): for example, parenthesized braids with specified bottom and top parenthetizations form one space, so do knottings of a given trivalent graph (skeleton). There is also a large collection of operations, consisting of all the internal operations of *uPaB*, *sKTG* and $\widetilde{wTF}$, as well as the maps a and cl.

In Sections 2.1 to 2.3 of [WKO2]we discuss associated graded structures and expansions for general algebraic structures. For any algebraic structure (think braids, or tangles with tangle composition), one allows formal linear compositions of elements of the same *kind* (think, same skeleton). Associated graded structures are taken with respect to the filtration by powers of the *augmentation ideal*. For the spaces *uPaB*, *sKTG* and $\widetilde{wTF}$, the associated graded spaces $\mathcal{A}^{hor}$, $\mathcal{A}^{u}$ and $\mathcal{A}^{sw}$ are the spaces of "horizontal chord diagrams on parenthesized strands", "chord diagrams on trivalent skeleta", and "arrow diagrams", as described in [BN1], [WKO2, Section 4.6], and Section 2 of this paper, respectively. As a result, the associated graded structure of $\mathcal{K}$ is

$$\mathcal{A} := \{\mathcal{A}^{hor} \xrightarrow{\text{cl}} \mathcal{A}^{u} \xrightarrow{\alpha} \mathcal{A}^{sw}\},$$

where cl and α are the maps induced by cl and a, respectively. More specifically, cl is the "closure of chord diagrams", and α is "replacing each chord with the sum of its two possible orientations", see [WKO2, Section 3.3].

An expansion [WKO2, Section 2.3] is a filtration-respecting map from an algebraic structure to its associated graded structure, whose associated graded map is the identity. In knot theory, expansions are also called universal finite type invariants. A homomorphic expansion is an expansion which behaves well with respect to the operations of the algebraic structure, that is, it intertwines each operation with its induced counterpart on the associated graded structure; for a detailed definition and introduction see [WKO2, Section 2.3]. Hence, a homomorphic expansion $Z : \mathcal{K} \to \mathcal{A}$ is a triple of homomorphic expansions Z^b, Z^u, and Z^w for $\mathcal{K}^b := uPaB$, $\mathcal{K}^u := sKTG$ and $\mathcal{K}^w := \widetilde{wTF}$, respectively, so that the following diagram commutes:

$$\begin{array}{ccccccc} \mathcal{K}: & & \mathcal{K}^b & \xrightarrow{\text{cl}} & \mathcal{K}^u & \xrightarrow{a} & \mathcal{K}^w \\ & {\scriptstyle Z}\downarrow & \downarrow{\scriptstyle Z^b} & & \downarrow{\scriptstyle Z^u} & & \downarrow{\scriptstyle Z^w} \\ \mathcal{A}: & & \mathcal{A}^{hor} & \xrightarrow{\text{cl}} & \mathcal{A}^{u} & \xrightarrow{\alpha} & \mathcal{A}^{w} \end{array} \tag{2}$$

We recall (see [BN1]) that a homomorphic expansion Z^b for parenthesized braids is determined by a "horizontal chord associator" $\Phi = Z^b(|\nearrow|)$. A homomorphic expansion Z^u of *sKTG* is also determined[2] by a Drinfel'd associator (horizontal chords or not; see [WKO2, Section 4.6]), so the significance of the left commutative square is to force the associator corresponding to Z^u to be a horizontal chord associator. In turn, Z^w is determined by a solution F (a close cousin of $V = Z^w(\curvearrowright)$) to the Kashiwara-Vergne problem (see [WKO2, Section 4.4 – 4.5]). The goal of this paper is to prove the following theorem, which, via the correspondence above, implies the KV conjecture:

Theorem 1.1. (1) *Assuming that $Z : \mathcal{K} \to \mathcal{A}$ exists, it is determined*[3] *by Z^u.*

(2) *There is a formula for $V = Z^w(\curvearrowright)$ and $C = Z^w(\downarrow)$ in terms of the Drinfel'd associator Φ associated to Z^u:*

$$V = C_1^{-1}C_2^{-1}C_{(12)}\varphi\left(\Phi^{-1}(a_{2(13)}, -a_{2(13)} - a_{4(13)}) \cdot e^{a_{23}/2}\Phi(a_{23}, a_{43})\right), \tag{3}$$

[2]With the exception of some minor normalization, see [WKO2], Lemma 4.14 and the paragraph after.

[3]In fact, almost entirely determined by Z^b, with the exception of some minor normalization of Z^u which is not determined by an associator.

where a denotes a single arrow[4]*. This agrees*[5] *with the formula proven in* [AET].

(3) *Every Z^b extends to a Z.*

The key to the proof of the theorem is to show that the generator $\nearrow_{\searrow}$ of $\widetilde{wTF}$ can be expressed in terms of the generator $|\nearrow|$ of $uPaB$ and the operations of $\mathcal{K}$. Assuming that Z exists, this yields a formula for V in terms of Φ.

1.3. **Paper Structure.** In Section 2 we provide an overview of the space wTF^o of (oriented) w-foams and its extension with strings $\widetilde{wTF}$. We provide a brief review of definitions and crucial facts from [WKO2], and details of the extension. We prove that homomorphic expansions for wTF^o extend uniquely to homomorphic expansions for $\widetilde{wTF}$.

Section 3 makes up the bulk of the paper and is devoted to the proof of Theorem 1.1. In Section 3.1 we prove part (1). In Section 3.2 we deduce the formula for Kashiwara-Vergne solutions in terms of Drinfel'd associators, proving part (2). In Section 3.3 we prove statement (3), the hardest part of the proof.

Section ?? is a short section of closing remarks, and in Appendix A we give an explicit comparison and equivalence between our formula in Part (2) and the ALekseev–Enriquez–Torossian [AET] formula.

2. The spaces $\widetilde{wTF}$ and $\mathcal{A}^{sw}$ in more detail

As mentioned in the introduction, $\widetilde{wTF}$ is a minor extension of the space wTF^o studied in [WKO2, Section 4.1 – 4.4]. It can be introduced as a planar algebra or as a circuit algebra; we will do the latter as it is simpler and more concise. Circuit algebras are defined in [WKO2, Section 2.4]; in short, they are similar to planar algebras but without the planarity requirement for "connecting strands". As in [WKO2], each generator and relation of $\widetilde{wTF}$ has a local topological interpretation. Recall from [WKO2, Sections 1.2, 3.4, 4.1] that wTF^o diagrams represent certain ribbon knotted tubes with foam vertices in $\mathbb{R}^4$, and the circuit algebra wTF^o is conjecturally a Reidemeister theory for this space (i.e., there is a surjection δ from the circuit algebra wTF^o to ribbon knotted tubes with foam vertices, and δ is conjectured to be an isomorphism). The space $\widetilde{wTF}$ extends wTF^o by adding one-dimensional strands to the picture. Note that in themselves, one dimensional strands in $\mathbb{R}^4$ are never knotted, however, they can be knotted *with* the two-dimensional tubes. In figures two-dimensional tubes will be denoted by thick lines and one dimensional strings by thin red lines. With this in mind, we define $\widetilde{wTF}$ as a circuit algebra defined in terms of generators and relations, and with some extra operations beyond circuit algebra compositions. Each generator, relation and operation has a local topological interpretation which provides much of the intuition behind the proofs. However, the corresponding Reidemeister theorem is only conjectural.

$$\widetilde{wTF} = \mathrm{CA}\Big\langle \underbrace{\;\;,\;\;,\;\;,\;\;,\;\;,\;\;,\;\;,\;\;,\;\;}_{\text{generators}} \;\Big|\; \begin{array}{c}\text{relations}\\ \text{as in}\\ \text{Section 2.2}\end{array} \;\Big|\; \begin{array}{c}\text{auxiliary}\\ \text{operations as}\\ \text{in Section 2.3}\end{array} \Big\rangle$$

[4]The notation is explained in detail in Section 3.2

[5]Although the two formulas are written in different languages, and checking that they agree takes effort. See Section 3.2 and Appendix A.

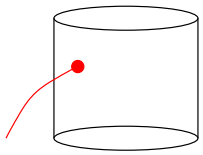

Figure 2. A string-tube vertex. fig:MixedV

bsec:wgens

2.1. **The generators of $\widetilde{wTF}$.** We begin by discussing the local topological meaning of each generator shown above.

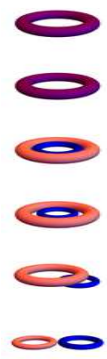

The first five generators are as described in [WKO2, Sections 4.1.1], we briefly recall their descriptions here. Knotted (more precisely, braided) tubes in $\mathbb{R}^4$ can equivalently be thought of as movies of flying rings in $\mathbb{R}^3$. The two crossings stand for movies where two rings trade places by the ring of the under strand flying through the ring of the over strand. The dotted end represents a tube "capped off" at the bottom by a disk. Generators 4 and 5 stand for singular "foam vertices", and will be referred to as the positive and negative vertex, respectively. The positive vertex represents the movie shown on the left: the right ring approaches the left ring from below, flies inside it and merges with it. The negative vertex represents a ring splitting and the inner ring flying out below and to the right. To be completely precise, $\widetilde{wTF}$ as a circuit algebra has more vertex generators than shown above: the vertices appear with all possible orientations of the strands. However, all other versions can be obtained from the ones shown above using "orientation switch" operations (to be discussed in Section 2.3). subsec:wops

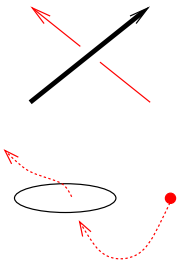

The thin red strands denote one dimensional strings in $\mathbb{R}^4$, or "flying points in $\mathbb{R}^3$". The crossings between the two types of strands (generators 6 and 7) represent "points flying through rings". For example, the picture on the left shows generator 6, where "the point on the right approaches the ring on the left from below, flies through the ring and out to the left above it". This explains why there are no generators with a thick strand crossing under a thin red strand: a ring cannot fly through a point.

Generator 9 is a trivalent vertex of 1-dimensional strings in $\mathbb{R}^4$. Finally, the last generator is a *mixed vertex:* a one-dimensional string attached to the wall of a 2-dimensional tube, as shown in Figure 2. All generators should be shown in all possible strand orientation combinations; we are suppressing this to save space. fig:MixedVertex

bsec:wrels

2.2. **The relations.** As a list, the relations for $\widetilde{wTF}$ are the same as the relations for wTF^o [WKO2, Section 4.5]: {R1^s, R2, R3, R4, OC, CP}. Recall that R1^s is the weak (framed) version of the Reidemeister 1 move; R2 and R3 are the usual second and third Reidemeister moves; R4 allowes moving a strand over or under a vertex. OC stands for *Overcorssings Commute*, CP for *Cap Pullout*: these two relations are shown in Figure 3, for a detailed explanation see [WKO2, Section 4.1.2]. fig:wTFeqels

In $\widetilde{wTF}$ all relations should be interpreted in all possible combinations of strand types and orientations (tube or string), for example the lower strand of the R2 relation can either be thick black or thin red, as shown below:

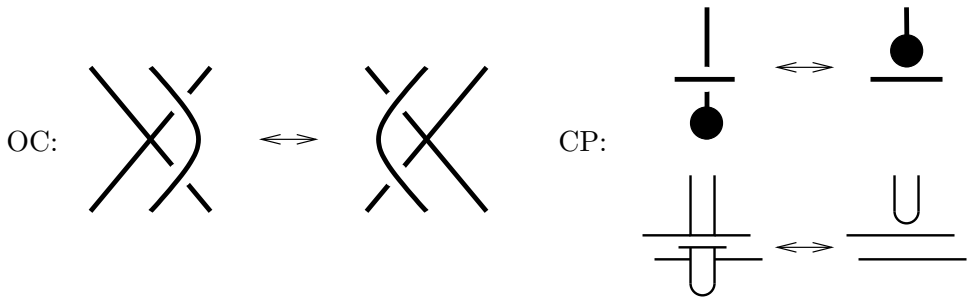

Figure 3. The OC and CP relations.

fig:wTFeRe

Similarly, any of the lower strands of the R3, R4, and OC relations may be thin red.

As in wTF^o, the relations all have local topological meaning and conjecturally $\widetilde{wTF}$ is a Reidemeister theory for ribbon knotted tubes in $\mathbb{R}^4$ with caps, singular foam vertices and attached strings. For example, Reidemeister 2 with a thin red bottom strand is imposed because the movie where a point flies in through a ring and then immediately flies back out is isotopic to the movie where there is no interaction between the point and ring at all.

It is easy to verify that all relations represent local isotopies of welded (ribbon knotted) tubes in $\mathbb{R}^4$ with singular vertices and attached strings. What is not clear at this stage is that this is a complete Reidemeister theory, that is, whether this is a complete set of relations. For more detail on this see [WKO2, Section 1.2].

Bar-NatanDancso:WKO2

ubsec:wops

2.3. **The operations.** Like wTF^o, $\widetilde{wTF}$ is equipped with a set of auxiliary operations in addition to the circuit algebra structure.

The first of these is orientation reversal. For the thin (red) strands, this simply means reversing the direction of the strand. For the thick strands (tubes), orientation switch comes in two versions. Recall from [WKO2, Section 3.4] that in the topological interpretation of wTF^o, each tube is oriented as a 2-dimensional surface, and also has a distinguished "core": a line along the tube which is oriented as a 1-dimensional manifold and determines the "direction" or "1-dimensional orientation" of the tube. Both of these are determined by the direction of the strand in the circuit algebra, via Satoh's tubing map.

Bar-NatanDancso:WKO2

Topologically, the operation "orientation switch", denoted S_e for a given strand e, acts by reversing both the (1-dimensional) direction and the (2-dimensional) orientation of the tube e. Diagrammatically, this corresponds to simply reversing the direction of the corresponding strand e.

The "adjoint" operation, denoted A_e, on the other hand only reverses the (1-dimensional) direction of the tube e, not the orientation as a surface. Diagrammatically, this manifests itself as reversing the strand direction and adding two virtual crossings on either side of each crossing where e crosses *over* another strand, as shown on the right (note that the strand below e may be thick

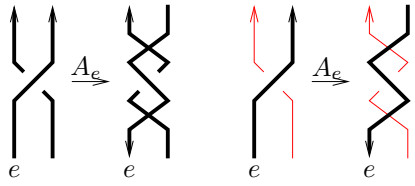

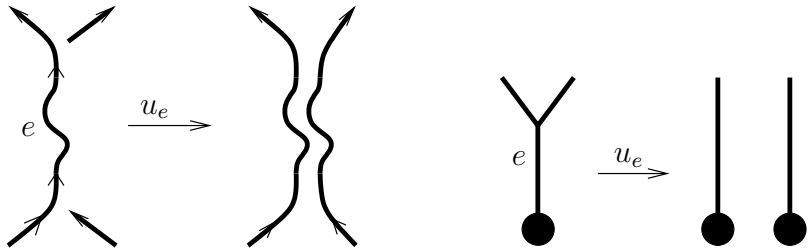

Figure 4. Unzip and disc unzip.

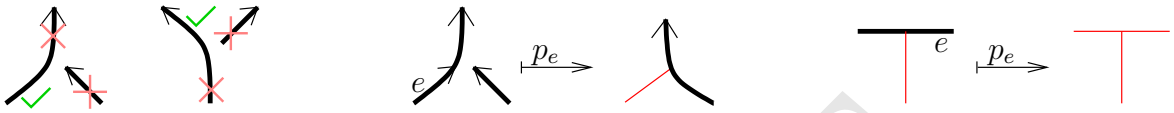

Figure 5. Puncture operations: the picture on the left shows which edges can be punctured at each vertex. The middle and right pictures show the effect of puncture operations.

or thin). Note that virtual crossings don't appear when e crosses under another strand. For more details on orientations and orientation switches, see [WKO2, Sections 3.4 and 4.1.3].

The unzip operation u_e doubles the strand e using the blackboard framing, and then attaches the ends of the doubled strand to the connecting ones, as shown in Figure 4. We restrict unzip to strands whose two ending vertices are of different signs. (For the definition of crossing and vertex signs, see [WKO2, Sections 3.4 and 4.1].) Topologically, the blackboard framing of the diagram induces a framing of the corresponding tube in $\mathbb{R}^4$ via Satoh's tubing map, and unzip is the act of "pushing the tube off of itself slightly in the framing direction". Note that unzips preserve the ribbon property.

A related operation, *disc unzip*, is unzip done on a capped strand, pushing the tube off in the direction of the framing (in diagram world, in the direction of the blackboard framing), as before. An example is shown in Figure 4; see [WKO2, Section 4.1.3] for details on framings and unzips.

So far all the operations we have introduced had already existed in wTF^o. There is also a new operation is called "puncture", denoted p_e, which diagrammatically simply turns the thick black strand e into a thin red one. The corresponding topological picture is "puncturing a tube", i.e., removing a small disk from it and retracting the rest to its core. Any crossings where e passes under another strand are not affected, while crossings in which e is the over strand turn into virtual crossings.

For simplicity, we place a restriction on which strands can be punctured, namely at each (fully thick black) vertex puctures are only allowed for one of the three meeting strands, as shown on the left of Figure 5. More general puctures could be allowed in a theory with more than one kind of "string to tube" vertex. The right of the same figure shows that when puncturing one of the thick strands of a mixed vertex, the puncture "spreads". Topologically, this is because the mixed vertex represents a string attached to a tube, so when puncturing e, the entire tube retracts to its core. Finally, a capped tube disappears (deformation retracts to a point) when punctured.

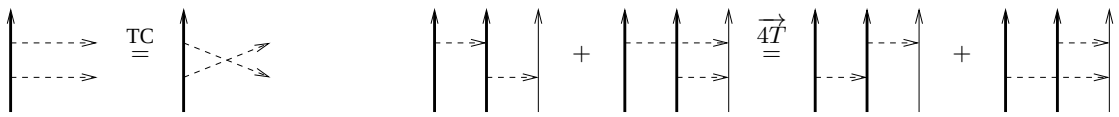

Figure 6. The TC and $\overrightarrow{4T}$ relations. Note that the 3rd strand in each term of the $\overrightarrow{4T}$ relation can be either thick black or thin red, the relation applies in either case.

fig:TCand4

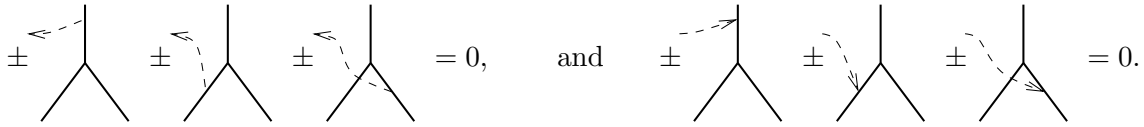

Figure 7. The VI relation: the vertices and strands could be of any type, but the same throughout the relation.

fig:VI

In summary,

$$\widetilde{wTF} = \mathrm{CA}\left\langle \underbrace{1, 2, 3, 4, 5, 6, 7, 8, 9}_{\text{generators}} \;\middle|\; \begin{array}{c}\mathrm{R1}^s,\ \mathrm{R2},\ \mathrm{R3},\\ \mathrm{R4},\ \mathrm{OC},\ \mathrm{CP}\\ \text{relations}\end{array} \;\middle|\; \begin{array}{c}S_e, A_e, u_e, d_e, p_e\\ \text{auxiliary}\\ \text{operations}\end{array} \right\rangle$$

2.4. **The associated graded structure $\mathcal{A}^{sw}$.** As in [WKO2], the space $\widetilde{wTF}$ is filtered by powers of the augmentation ideal and its associated graded space, denoted $\mathcal{A}^{sw}$, is a "space of arrow diagrams on foam skeletons with strings". As a circuit algebra, $\mathcal{A}^{sw}$ is presented as follows:

Bar-NatanDancso:WKO2

$$\mathcal{A}^{sw} = \mathrm{CA}\left\langle \underbrace{1, 2, 3, 4, 5, 6, 7}_{\text{generators}} \;\middle|\; \begin{array}{c}\text{relations}\\ \text{as below}\end{array} \;\middle|\; \begin{array}{c}\text{auxiliary}\\ \text{operations}\\ \text{as below}\end{array} \right\rangle.$$

Generators 1 and 5 are called single arrows and they are of degree one, while all others are "skeleton features" of degree zero. The relations are almost the same as in [WKO2, Section 4.2.1], which describes the relations for the associated graded of wTF^o: $\overrightarrow{4T}$ (the 4-Term relation), TC (Tails Commute), RI (Rotation Invariance), CP (the arrow Cap Pullout), and VI (Vertex Invariance). For $\widetilde{wTF}$ there is an additional relation TF (Tails Forbidden on strings). The TC and $\overrightarrow{4T}$ relations are shown in Figure 6. The Vertex Invariance relation is shown in Figure 7: here the $\pm$ signs depend on the strand orientations. Note that the type of the vertex and the types of each strand (thick black or thin red) are left undetermined: the VI relation applies in all cases. Figure 8 shows the other relations: RI, CP and TF. Note that technically TF is not a relation: there were no generators with an arrow tail on a thin red strand, so saying that such an element vanishes is meaningless. However, without TF the VI relation would have to be stated for all the sub-cases of 0, 1 or 3 thin red strands, so we prefer this cleaner way, even if it is a slight abuse of notation.

Bar-NatanDancso:WKO2

fig:TCand4T

fig:VI

fig:RICPTF

Each operation on $\widetilde{wTF}$ induces a corresponding operation on $\mathcal{A}^{sw}$. Orientation switch, adjoint, unzip, cap unzip, and long strand deletion act exactly the same way as they do

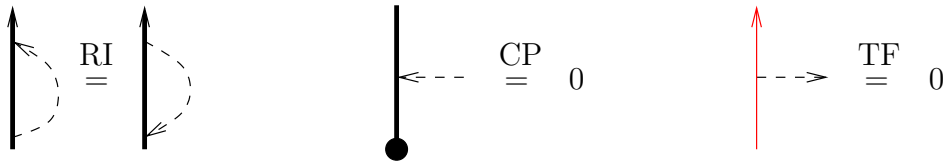

Figure 8. The RI and CP relations, and the TF relation (which is not really a relation). fig:RICPTF

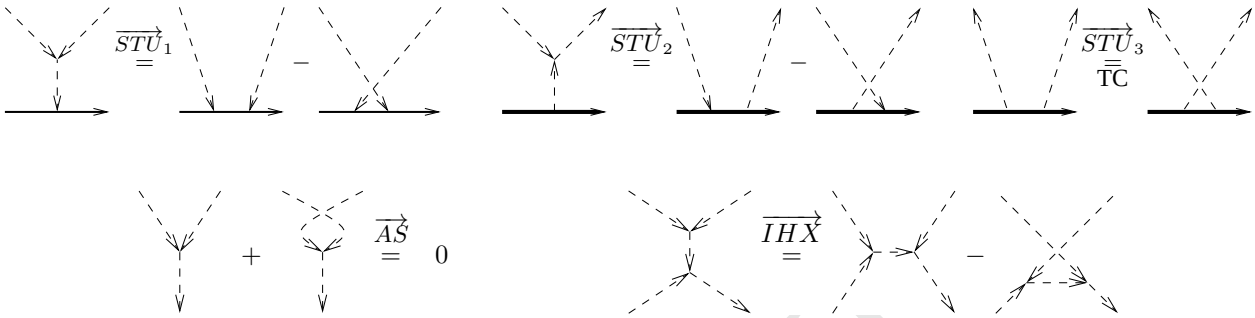

Figure 9. The $\overrightarrow{AS}$, $\overrightarrow{IHX}$ and the three $\overrightarrow{STU}$ rerations. Note that in $\overrightarrow{STU}_1$, the skeleton strand can be thin red or thick black, and that $\overrightarrow{STU}_3$ is the same as the TC relation. fig:ASIHXS

for wTF^{oo}. We quickly recall these here, for details see [WKO2, Section 4.2.2]. The orientation switch S_e reverses the orientation of the skeleton strand e, and multiplies the arrow diagram by $(-1)^{\#\{\text{arrow heads and tails on } e\}}$. The adjoint operation also reverses the skeleton strand e and multiplies the arrow diagram by $(-1)^{\#\{\text{arrow heads on } e\}}$. Given a skeleton S with a distinguished strand e, unzip (or disc unzip, if e is capped) is an operation $u_e : \mathcal{A}^{sw}(S) \to \mathcal{A}^{sw}(u_e(S))$ which maps each arrow ending on e to a sum of two arrows, one ending on each of the two new strands which replace e. Deleting a long strand e kills all arrow diagrams with any arrow ending on e. The operation induced by puncture, denoted p_e, turns the formerly thick black e into a thin red strand, and kills any arrow diagram with any arrow tails on e.

To summarise:

$$\mathcal{A}^{sw} = \mathrm{CA}\left\langle \underbrace{1, 2, 3, 4, 5, 6, 7}_{\text{generators}} \;\middle|\; \begin{array}{c}\overrightarrow{4T},\ \mathrm{TC},\ \mathrm{VI},\\ \mathrm{CP},\ \mathrm{RI},\ \mathrm{TF}\\ \text{relations}\end{array} \;\middle|\; \begin{array}{c}S_e, A_e, u_e, d_e, p_e\\ \text{auxiliary}\\ \text{operations}\end{array} \right\rangle$$

As in [WKO2, Definition 3.7], we define a "w-Jacobi diagram" (or just "arrow diagram") by also allowing trivalent chord vertices, each of which is equipped with a cyclic orientation, and modulo the $\overrightarrow{STU}$ relations of Figure 9. Denote the circuit algebra of formal linear combinations of these w-Jacobi diagrams by $\mathcal{A}^{swt}$. Then, as in [WKO2, Theorem 3.8], we have the following "bracket-rise" theorem:

Theorem 2.1. *The natural inclusion of diagrams induces a circuit algebra isomorphism $\mathcal{A}^{sw} \cong \mathcal{A}^{swt}$. Furthermore, the $\overrightarrow{AS}$ and $\overrightarrow{IHX}$ relations of Figure 9 hold in $\mathcal{A}^{swt}$.*

The proof is identical to the proof of [WKO2, Theorem 3.8]. In light of this isomorphism, we will drop the extra "t" from the notation and use $\mathcal{A}^{sw}$ to denote either of these spaces. As in [WKO2], the primitive elements of $\mathcal{A}^{sw}$ are connected diagrams, denoted $\mathcal{P}^{sw}$, and

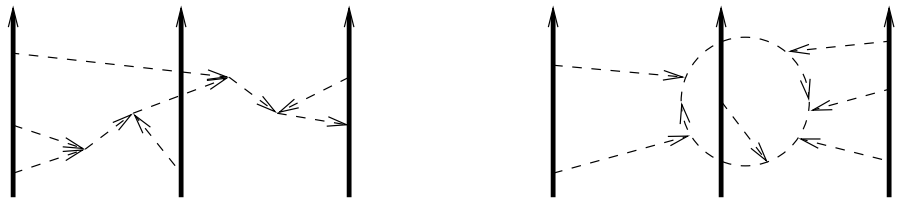

Figure 10. An example of a *tree*, left, and a *wheel*, right.

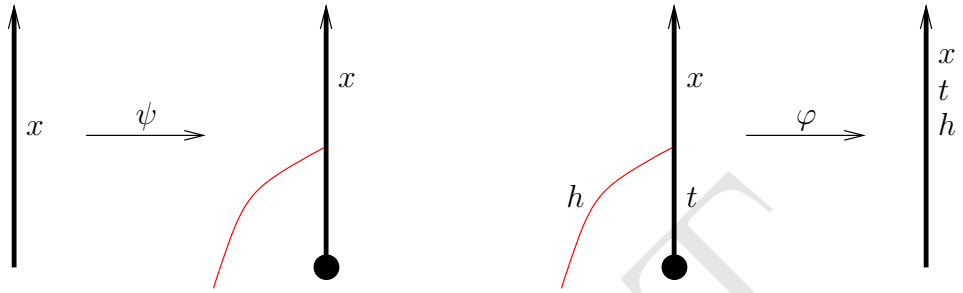

Figure 11. Inverse maps.

$\mathcal{P}^{sw} = \{\text{trees}\} \oplus \{\text{wheels}\}$ as a vector space. Examples of trees and wheels are shown in Figure 10; for details see [WKO2, Section 3.1]. Note that the RI relation can now be rephrased (via $\overrightarrow{STU}_2$) as the vanishing of the wheel with a single spoke, or one-wheel.

We recall the following two crucial facts [WKO2, Lemmas 4.6 and 4.7]:

Fact 2.2. *$\mathcal{A}^{sw}(\downarrow)$, the part of $\mathcal{A}^{sw}$ with skeleton a single capped strand, is isomorphic as a vector space to the completed polynomial algebra freely generated by wheels w_k with $k \geq 2$.*

Fact 2.3. *$\mathcal{A}^{sw}(\nearrow_{\nwarrow}) \cong \mathcal{A}^{sw}(\uparrow_2)$, where $\mathcal{A}^{sw}(\nearrow_{\nwarrow})$ stands for the space of arrow diagrams whose skeleton is a single vertex (the picture shows a positive vertex but the statement is true for all kinds of vertices with thick black strands), and $\mathcal{A}^{sw}(\uparrow_2)$ is the space of arrow diagrams on two (thick black) strands.*

The following Lemma – called the *Sorting Lemma* as we will see it "sorts" arrow tails above arrow heads – will play an important role. In particular the second isomorphism stated is the map φ appearing in Theorem 1.1, part (2). We will refer to the isomorphism φ of the Lemma as the *sorting isomorphism*.

Lemma 2.4 (Sorting Lemma)**.** *There is a linear isomorphism $\varphi : \mathcal{A}^{sw}\left(\right.$  $\left.\right) \xrightarrow{\cong} \mathcal{A}^{sw}(\uparrow)$ between the vector spaces of arrow diagrams on the indicated skeleta. On the left, the thin red string is a tangle end. The black strand may continue past the arrow, and there may be additional skeleton components: the same on both sides. Applying the isomorphism φ twice, one obtains $\mathcal{A}^{sw}\left(\right.$  $\left.\right) \overset{\varphi}{\cong} \mathcal{A}^{sw}(\uparrow_2)$.*

Proof. We construct inverse maps between the two spaces. There is a natural map $\mathcal{A}^{sw}(\uparrow) \xrightarrow{\psi} \mathcal{A}^{sw}\left(\right.$ $\left.\right)$, shown in Figure 11: given an arrow diagram on a single thick black strand, place all arrow endings (denoted "x") on the strand above the tube/string vertex.

In the other direction, consider an arrow diagram on the capped/stringed vertex. One may assume that there are only arrow tails on the capped strand under the vertex: any arrow head may be commuted using $\overrightarrow{STU}$ relations towards the cap, where it is killed by the CP relation[6]. On the thin red strand there are only arrow heads. To construct φ, first "push" the arrow tails (denoted "t") from the capped strand up across the vertex using the VI relation. Since tails vanish on the thin red strand, they simply slide past the vertex. Once the capped side is cleared, continue by sliding the arrow heads "h" up from the thin red string to the strand above the vertex. Now the cap relation kills any arrow heads on the capped strand, so once again they simply slide past the vertex. The result placed on a single thick black strand is shown in Figure 11.

It is clear that ψ is well-defined, we leave it to the reader to check that so is φ as a short exercise. Given that both maps are well-defined, it is clear that they are inverses of each other. □

Observe that in the image of φ, all arrow tails are above arrow heads along the strand. Arrow diagrams of this form appear in the context of "over-then-under" tangles, which have applications in several contexts, including virtual braid classification [BDV].

2.5. **The homomorphic expansion.** As discussed in [WKO2, Section 2.3], an expansion for $\widetilde{wTF}$ is a map $Z^w : \widetilde{wTF} \to \mathcal{A}^{sw}$ with the property that the associated graded map $\operatorname{gr} Z^w : \mathcal{A}^{sw} \to \mathcal{A}^{sw}$ is the identity map $\mathrm{id}_{\mathcal{A}^{sw}}$. A homomorphic expansion is an expansion which also intertwines each operation of $\widetilde{wTF}$ with its arrow diagrammatic counterpart. In [WKO2, Theorems 4.9 and 4.11] we proved that the existence of solutions for the Kashiwara–Vergne equations implies that there exsists a homomorphic expansion for wTF^o. In fact that homomorphic expansions[7] for wTF^o are in one-to-one correspondence with solutions to the Kahiwara-Vergne problem.

The point of this paper is to provide a topological construction for such a homomorphic expansion (and hence for a solution of the Kashiwara–Vergne conjecture), and this is easier to do for the slightly more general space $\widetilde{wTF}$.

Let $\mathcal{A}^{osw} \subseteq \mathcal{A}^{sw}$ denote arrow diagrams on wTF^o skeleta, the associated graded space of wTF^o. One of the key results of [WKO2, Section 4.3] is the characterisation of homomorphic expansions of wTF^o. For any (group-like) homomorphic expansion $Z^{ow} : wTF^o \to \mathcal{A}^{osw}$, the value $Z^{ow}(\nwarrow\!\!\nearrow)$ is uniquely determined and equals $R = e^{a_{12}}$, where a_{12} denotes a single arrow from the over strand 1 to the under strand 2.

To state the full characterisation, we use co-simplicial notation in subscripts. For example, for $R = e^{a_{12}} =\in \mathcal{A}^{sw}(\uparrow_2)$, $R_{13} = e^{a_{13}}$ and $R_{23} = e^{a_{23}}$ in $\mathcal{A}^{sw}(\uparrow_3)$ are the diagrams where R is placed on strands 1 and 3, and 2 and 3, respectively. $R_{(12)3} \in \mathcal{A}^{sw}(\uparrow_3)$ is obtained by doubling the first strand of R and placing it on strands 1 and 2, and placing the second strand of R on strand 3, that is, $R_{(12)3} = e^{a_{13}+a_{23}}$. Similarly for $V \in \mathcal{A}(\uparrow_2)$, $V_{12} \in \mathcal{A}(\uparrow_3)$ denotes V placed on the first two starnds, et cetera.

Fact 2.5. *A filtered, group-like map $Z^{ow} : wTF^o \to \mathcal{A}^{osw}$ is a homomorphic expansion if and only if the Z^{ow}-values $V = Z^{ow}(\nearrow\!\!\searrow)$ and $C = Z^{ow}(\bullet\!\!\downarrow)$ satisfy the following equations:*

(1) R4 Equation*:*

$$V_{12}R_{(12)3} = R_{23}R_{13}V_{12} \quad \text{in } \mathcal{A}^{sw}(\uparrow_3). \tag{R4}$$

[6]This argument also appears in [WKO2], for example as the basic idea for the proof of Fact 2.2.

[7]Subject to the minor technical condition that the value of the vertex doesn't contain isolated arrows.

(2) Unitarity Equation:

$$V \cdot A_1 A_2(V) = 1 \quad \text{in } \mathcal{A}^{sw}(\uparrow_2), \tag{U}$$ eq:U

where A_1 and A_2 denote the antipode operations.

(3) Cap Equation[8]:

$$C_{(12)} V_{12}^{-1} = C_1 C_2 \quad \text{in } \mathcal{A}^{sw}(\downarrow_2), \tag{C}$$ eq:C

where the subscripts mean strand placements as in the R4 Equation.

We begin by showing that finding a homomorphic expansion for $\widetilde{wTF}$ is no harder than finding one for wTF^o.

ndRestrict **Theorem 2.6.** *Homomorphic expansions for wTF^o are in one-to-one correspondence with homomorphic expansions for $\widetilde{wTF}$ via unique extension and restriction.*

Proof. Every element of wTF^o is also in $\widetilde{wTF}$, hence any Z^w restricts to a homomorphic expansion Z^{ow} of wTF^o. Every element of $\widetilde{wTF}$ is the result of puncturing – possibly on multiple strands – an element of wTF^o, and Z^w is required to commute with punctures. Hence any Z^{ow} uniquely extends to a Z^w. □

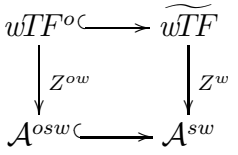

In [WKO2, Section 4.4] we showed that short arrows – arrows whose head and tail is not separated by any other arrow endings – supported on either strand of V don't affect whether Z^w is a homomorphic expansion. That is, if Z^w is a homomorphic expansion and a is a linear combination of short arrows, then replacing V by $e^a V$ gives rise to another homomorphic expansion. Hence, in [WKO2] we typically assume there are no short arrows in V, this motivates the following definition:

Definition 2.7. A homomorphic expansion Z is *v-small* if there are no short arrows in the Z-value V of the positive vertex.

As it turns out, the value of the left-punctured vertex is trivial under any v-small homomorphic expansion. This fact will be useful later, so we prove it here.

lem:pV **Lemma 2.8.** *For any v-small homomorphic expansion Z^w, $Z^w\left($  $\right) = 1$, that is, the Z^w-value of a left punctured vertex is trivial.*

Proof. Recall from [WKO2, Proof of Theorem 4.9] that the Z^w-value V of the positive (not punctured) vertex can be written as $V = e^b e^t$, where b is a linear combination of wheels only and t (denoted uD in [WKO2]) is a linear combination of trees. Puncturing the left strand of V kills all arrow diagrams with tails on the left strand. Diagrams that survive are wheels, and trees all of whose tails are on the right side strand. However, if all tails of a tree are supported on one strand, then the tree is a single arrow, due to TC and the anti-symmetry of the trivalent arrow vertices, thus the only surviving trees are simple arrows directed from right to left. Observe that all of these arrow diagrams commute with each other in $\mathcal{A}^{sw}(\uparrow_2)$.

Denote the value of the punctured vertex by $p_1 V = e^{p_1(b)} e^{p_1(t)}$. Recall that V must satisfy the Unitarity Equation of Fact 2.5, so $p_1 V \cdot A_1 A_2(p_1 V) = 1$. Since wheels have only tails,

[8] For convenience we state the Cap Equation phrased for caps at the bottom of strands, hence the difference from the equivalent formulation in [WKO2].

$A_1A_2(p_1(b)) = p_1(b)$. Each arrow has one head, so $A_1A_2(p_1(t)) = -p_1(t)$. Hence, using commutativity, $p_1V \cdot A_1A_2(p_1V) = e^{2p_1(b)} = 1$, which implies that $p_1(b) = 0$. As for $p_1(t)$, one can show that there are no arrows pointing from the right to the left strand by a direct computation in degree 1. □

3. Proof of Theorem 1.1

3.1. Proof of Part (1).

We prove Part 1 in two steps: first verifying the easier "tree level" case, which nonetheless contains the main idea, then in general.

3.1.1. *Tree level proof of Part (1).* Let $\mathcal{A}^{tree}$ denote the quotient of $\mathcal{A}^{sw}$ by all wheels, and let $\pi : \mathcal{A}^{sw} \to \mathcal{A}^{tree}$ denote the quotient map (cf [WKO2, Section 3.2]). Part (1) of the main theorem is the same as stating that Z^w is determined by Z^u. Z^w, in turn is determined by the values V and C of the positive vertex and the cap [WKO2, Sections 4.3 and 4.5], so one only needs to show that V and C are determined by Z^u. Proving this "on the tree level" means showing only that $\pi(V)$ and $\pi(C)$ are determined by Z^u. In particular, observe that since C is a linear combination of products of wheels (Fact 2.2), we have $\pi(C) = 1$, so we only need to show that $\pi(V)$ is determined by Z^u.

Let B^u denote the "buckle" *sKTG*, as shown on the right (ignore the dotted lines for now). All edges are oriented up, and by the drawing conventions of [WKO2, Section 4.6] all the vertices in the bottom half of the picture are negative and all the ones in the top half are positive. Let $B^w = a(B^u) \in \widetilde{wTF}$, and $\beta^u := Z^u(B^u)$. Note that β^u can be thought of as a chord diagram on four strands: use VI relations to move all chord endings to the "middle" of the skeleton, between the dotted lines on the picture. Hence, we write $\beta^u \in \mathcal{A}^u(\uparrow_4)$. Let $\beta^w = \alpha(\beta^u)$, and note that by the compatibility of Z^u and Z^w we have $\beta^w = Z^w(B^w)$. We will perform a series of operations on B^w and $\pi(\beta^w)$ to recover $\pi(V)$ from it.

$B^u =$ 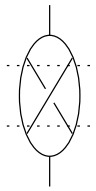

First, connect (a circuit algebra operation in $\widetilde{wTF}$) a positive vertex to the bottom of B^w, as shown in Figure 12. Then unzip the edge marked by u, and puncture the edges marked e and e'. Then attach a cap (once again a circuit algebra operation) to the thick black end at the bottom. Finally, unzip the capped strand.

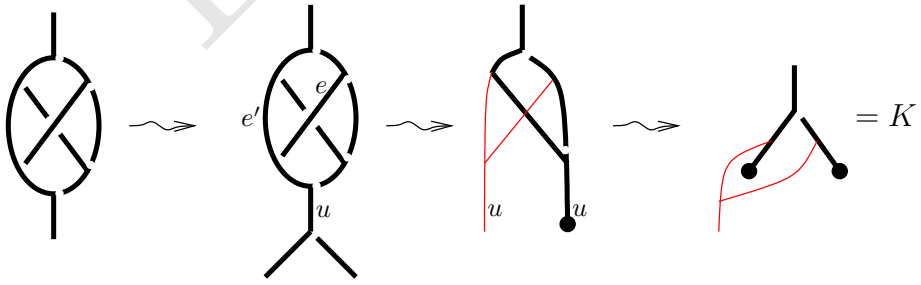

Figure 12. From the "buckle" β^w to the (modified) vertex.

Call the resulting w-foam K, as shown at the right in Figure 12. What is $Z^w(K)$? Due to the homomorphicity of Z, it is obtained from β^w by performing the same series of operations in the associated graded: a circuit algebra composition with V, unzip, punctures, circuit algebra composition with C, and disc unzip. Notice that the left strand of that attached

vertex got punctured, and hence by Lemma 2.8 the attached value V cancels.[9] $Z^w(K)$ still depends on the value C. At the tree level, since $\pi(C) = 1$, $\pi(Z^w(K))$ can be computed from β^w by performing punctures and unzips. Since $\beta^w = \alpha(\beta^u)$, this means that $\pi(Z^w(K))$ is determined by Z^u.

On the other hand, note that the space of chord diagrams on the skeleton of K is the space $\mathcal{A}(\uparrow_2)$ by Lemma 2.4 and VI. Note also that K is a circuit algebra combination of a vertex, two left-punctured right-capped vertices and an all-red-strings vertex, and the Z^w-values of the latter three are trivial. So $\pi(Z^w(K)) = \pi(V) \in \mathcal{A}^{tree}(\uparrow_2)$. Hence, $\pi(V)$ is determined by Z^u as needed. □

3.1.2. *Complete proof of Part (1).* In the previous subsection we showed that Z^u determines $\pi(V) \in \mathcal{A}^{tree}(\uparrow_2)$. The proof of Part (1) is completed by the following Lemma:

Lemma 3.1. *For any homomorphic expansion Z^w of $\widetilde{wTF}$, $V = Z^w(\nearrow\!\!\!\!\nwarrow)$ and $C = Z^w(\bullet\!\downarrow)$, $\pi(V) \in \mathcal{A}^{tree}(\uparrow_2)$ determines both V and C uniquely.*

Proof. We use a perturbative argument. By contradiction, assume this is not the case, in particular, first assume that there exist $V \neq V'$, both of which are vertex values of Z^u-compatible homomorphic expansions, such that $\pi(V) = \pi(V')$. Let v denote the lowest degree term of $V - V'$. Note that v is primitive and $v \in \ker \pi$, so v is a homogeneous linear combination of wheels. By the Unitarity Equation of Fact 2.5, we have $A_1A_2(v) = -v$. Recall that A_i reverses the direction of the strand i and multiplies each arrow diagram by (-1) to the number of heads on that strand. Since v has only tails, $A_1A_2(v) = v$, so $v = -v$, so $v = 0$, a contradiction. Therefore, $\pi(V)$ determines V uniquely.

Now we show that V determines C uniquely. Assume there are different values C and C' in $\mathcal{A}^{sw}(\bullet\!\downarrow)$ so that (V, C) and (V, C') are both vertex-cap value pairs of Z^u-compatible homomorphic expansions. Let c denote the lowest degree term of $C - C'$, then c is a scalar multiple of a single wheel. The Cap Equation of Fact 2.5 implies $c_{(12)} = c_1 + c_2$ in $\mathcal{A}^{sw}(\bullet\!\downarrow_2)$.

There is a well-defined linear map $\omega : \mathcal{A}^{sw}(\bullet\!\downarrow_2) \to \mathbb{Q}[x, y]$ sending an arrow diagram – which has arrow tails only on each strand – to "x to the power of the number of tails on strand 1, times y to the power of the number of tails on strand 2". Assume $c = \alpha w_r$, where w_r denotes the r-wheel, and $\alpha \in \mathbb{Q}$. Then $0 = \omega(c_{(12)} - c_1 - c_2) = \alpha((x + y)^r - x^r - y^r)$, so either $r = 1$ or $\alpha = 0$. But $w_1 = 0$ in $\mathcal{A}^{sw}$ by the RI relation, hence $\alpha = 0$ and thus $c = 0$, a contradiction. □

3.2. **Proof of Part (2).** In this section we compute V, the value of the vertex, from Φ, the Drinfel'd associator determining Z^b, using the construction of Part (1). In Appendix A we also show that this result translates to the [AET] formula for Kashiwara-Vergne solutions in terms of Drinfel'd associators.

In the computation of V from Φ, as well as later in the paper, we use two facts about Drinfel's associators. We summarise these in the following Lemma:

Lemma 3.2. *Let $\Phi = \Phi(c_{12}, c_{23}) \in \mathcal{A}^u(\uparrow_3)$ be a Drinfel'd associator, where c_{ij} denotes a chord between strands i and j. Then, the following facts hold for $\alpha(\Phi) \in \mathcal{A}^w(\uparrow_3)$:*

(1) *$p_ip_j\alpha(\Phi) = 1$, whenever $i, j \in \{1, 2, 3\}$, $i \neq j$, and p_i denotes puncture of the i-th strand.*

[9] Any short arrows would also cancel when the right strand is capped.

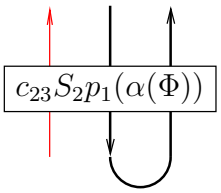

Figure 13. A concatenated associator.

(2) $c_{23}S_2p_1(\alpha(\Phi)) = 1$, *where* S_2 *stands for orientation switch of strand 2, and* c_{23} *is concatenation of strands 2 and 3 (a circuit algebra operation), as shown in Figure 13.*

Proof. To show Property (1), recall that is $\Phi(x, y)$ is a Drinfel'd associator, then, by the anti-symmetry property of associators, the image of Φ in the quotient where $xy = yx$ is 1. In particular, $\Phi(0, y) = \Phi(x, 0) = 0$.

Therefore $p_1p_2\alpha(\Phi) = 1$, because $p_1p_2\alpha(c_{12}) = p_1p_2(a_{12}+a_{21}) = 0$, therefore, $p_1p_2\alpha(\Phi) = 1$. The same reasoning shows that $p_2p_3\alpha(\Phi) = 1$.

Finally, $p_1p_3\alpha(\Phi(c_{12}, c_{23})) = \Phi(a_{21}, a_{23})$, and since $[a_{21}, a_{23}] = 0$ by the TC relation, $\Phi(a_{21}, a_{23}) = 1$.

For Property 2, note that $p_1(\alpha(\Phi)) = \Phi(a_{21}, -a_{21} - a_{31})$. Thus, strands 2 and 3 support only tails, and these commute by the TC relation, and $S_2p_1(\alpha(\Phi)) = \Phi(-a_{21}, a_{21} - a_{31})$. Furthermore, tails on strand 3 can be pulled to strand 2 through the concatenation, which identifies a_{21} with a_{31}. Therefore, $\Phi(-a_{21}, a_{21} - a_{31}) = \Phi(-a_{21}, 0) = 1$. □

To compute V and prove Part (2) of Theorem 1.1, consider once again the w-tangled foam K on the right of Figure 12.

On one hand, $Z^w(K)$ can be computed directly from the generators: $Z^w(K) = C_1C_2V_{12} \in \mathcal{A}^{sw}(\uparrow_2)$, since the values of the left-punctured vertices are trivial. Hence, if we know $Z^w(K)$, we know V.

On the other hand, we can compute $Z^w(K)$, using the compatibility with Z^u, as follows. Note that B^u is the closure – in the sense of (1) – of the parenthesised braid B^b shown in Figure 14, $B^w = a(B^u)$. Using the notation $\beta^u = Z^u(B^u)$, and $\beta^w = Z^w(B^w)$, and by the compatibility of Z^w with Z^u, we have

$$\beta^w = Z^w(B^w) = \alpha(Z^u(B^u)) = \alpha(\beta^u).$$

How does $Z^w(K)$ differ from β^w? To obtain K, a vertex and a cap were attached to B^w, two strands were punctured and the cap unzipped, as in Figure 12. The Z^w-value of the added vertex cancels when its left strand is punctured, however, the value of the cap remains and is unzipped. Thus, in loose notation, $Z^w(K) = u(C) \cdot p^2(\beta^w)$, where p^2 denotes the two punctures – we will compute this value explicitly in terms of associators shortly.

To equate the two approaches, we need to express $u(C) \cdot p^2(\beta^w)$ as an element of $\mathcal{A}^{sw}(\uparrow_2)$, by applying the *sorting isomorphism* φ of Lemma 2.4. By doing so, we obtain

$$C_1C_2V_{12} = \varphi(u(C)p^2(\beta^w)). \tag{4}$$

Through a careful analysis of the right hand side, this will imply formula (7) stated in Theorem 1.1. In summary, we want to compute

$$\Upsilon := \varphi(u(C)p^2(\beta^w)).$$

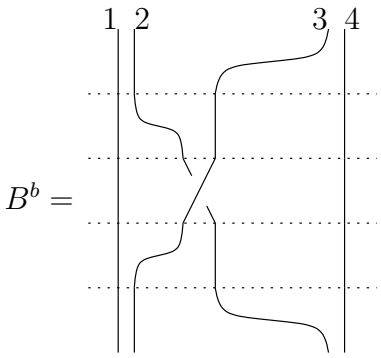

$$\begin{aligned}
\Phi_{(12)34} &\xmapsto{p^2\alpha} \Phi(a_{23}, a_{43}) \\
\Phi_{123}^{-1} &\longmapsto 1 \\
R_{32} &\longmapsto e^{a_{23}/2} \\
\Phi_{132} &\longmapsto 1 \\
\Phi_{(13)24}^{-1} &\longmapsto \Phi^{-1}(a_{2(13)}, -a_{2(13)} - a_{4(13)})
\end{aligned}$$

Figure 14. Computing β^b. Strands are numbered at the top and multiplication is read from bottom to top; the rightmost column lists the images of the factors under $p_1p_3\alpha$. fig:Buckle

To achieve this, we use that $\beta^w = \alpha(\beta^u)$, and compute β^u in terms of the Drinfel'd associator Φ associated to Z^u. By the compatibility of Z^u and Z^b, it is enough to compute $\beta^b := Z^b(B^b)$. The result can be read from the picture in Figure 14: fig:BuckleBraid

$$\beta^b = \Phi_{(13)24}^{-1}\Phi_{132}R_{32}\Phi_{123}^{-1}\Phi_{(12)34}.$$

Recall that the cosimplicial notation used in the subscripts show which strands the diagrams are placed on, for example, $\Phi_{(13)24}^{-1} = \Phi^{-1}(c_{12} + c_{32}, c_{24})$. Also recall that $R = e^{c/2}$, so $R_{32} = e^{c_{23}/2}$.

As β^u is the tree closure of β^b, it is given by the same formula interpreted as an element of $\mathcal{A}^u(\uparrow_4)$. One then applies α to obtain $\beta^w = \alpha(\beta^u)$. After the vertex and cap attachment, fig:Buckle101 of Figure 12, strands 1 and 3 are punctured and strands 2 and 4 are capped, and in this strand numbering, $u(C) = C_{24}$ Therefore, we have

$$\Upsilon = \varphi\left(C_{24} \cdot p_1p_3\alpha(\Phi_{(13)24}^{-1}\Phi_{132}R_{32}\Phi_{123}^{-1}\Phi_{(12)34})\right).$$

Next, we analyse how the puctures and α act on factors of β^b. First observe that $p_3\alpha(R_{32}) = e^{a_{23}/2}$, where a_{ij} is a single arrow pointing from strand i to strand j.

Observe that $p_1p_3\alpha(\Phi_{123}^{-1}) = p_1p_3\alpha(\Phi_{123}^{-1}) = 1$ by Fact (1) of Lemma 3.2. lt:TwoPuncturesasm:PhiFacts

Since strands 1 and 3 are both punctured, no arrows can be supported between these two strands, hence $p_1p_3\alpha(\Phi_{(12)34}) = \Phi(a_{23}, a_{43})$.

A basic property of associators is that $\Phi(x, y) = \Phi(x, -x - z)$ whenever $(x + y + z)$ is central. Using this property we deduce $\Phi_{(13)24}^{-1} = \Phi^{-1}(c_{(13)2}, c_{24}) = \Phi^{-1}(c_{(13)2}, -c_{(13)2} - c_{(13)4})$, so $p_1p_3\alpha\Phi_{(13)24}^{-1} = \Phi^{-1}(a_{2(13)}, -a_{2(13)} - a_{4(13)})$. To summarise,

$$\Upsilon = \varphi\left(C_{24} \cdot \Phi^{-1}(a_{2(13)}, -a_{2(13)} - a_{4(13)}) \cdot e^{a_{23}/2} \cdot \Phi(a_{23}, a_{43})\right).$$

Note that the expression $\Phi^{-1}(a_{2(13)}, -a_{2(13)} - a_{4(13)}) \cdot e^{a_{23}/2} \cdot \Phi(a_{23}, a_{43})$ has only arrow tails on strands 2 and 4, and therefore commutes with C_{24} by the TC relation. Hence, by the definition of φ,

$$\begin{aligned}
\Upsilon &= \varphi\left(\Phi^{-1}(a_{2(13)}, -a_{2(13)} - a_{4(13)}) \cdot e^{a_{23}/2} \cdot \Phi(a_{23}, a_{43}) \cdot C_{24}\right) \\
&= \varphi\left(\Phi^{-1}(a_{2(13)}, -a_{2(13)} - a_{4(13)}) \cdot e^{a_{23}/2} \cdot \Phi(a_{23}, a_{43})\right) \cdot \varphi(C_{24}).
\end{aligned}$$

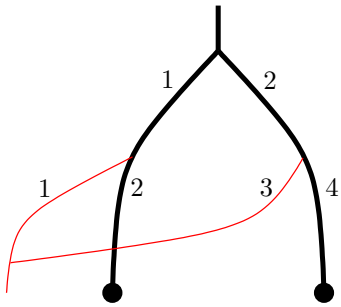

Figure 15. Strand numbering convention for K and V: arrow endings from strand 1 and 2 of K are "pushed" to strand 1 of V when applying φ, and arrow endings from strands 3 and 4 are pushed to strand 2.

Furthermore, by the strand numbering convention shown in Figure 15, we have $\varphi(C_{24}) = C_{12}$. Terefore,

$$V_{12} = C_1^{-1}C_2^{-1}\Upsilon = C_1^{-1}C_2^{-1}\varphi\left(\Phi^{-1}(a_{2(13)}, -a_{2(13)} - a_{4(13)}) \cdot e^{a_{23}/2} \cdot \Phi(a_{23}, a_{43})\right) C_{12},$$

as stated in part (2) of Theorem 1.1. □

Matching this result to the Alekseev–Enriquez–Torossian formula of [AET, Theorem 4.] is technical, and not used anywhere else in the paper, hence we defer this to Appendix A.

3.3. **Proof of part (3): the double tree construction.** Given a homomorphic expansion Z^u of *sKTG*, in Section 3.1.2 we showed that if there is to exist a homomorphic expansion Z^w of $\widetilde{wTF}$ compatible with Z^u, then $V = Z^w(\nearrow\!\!\!\!\searrow)$ and $C = Z^w(\,\downarrow)$, and hence Z^w itself, are uniquely determined by Z^u. From here on we denote these unique values – which arose from the "buckle" construction – by V_β and C_β, and the candidate homomorphic expansion determined by them Z^w_β.

It remains to prove that Z^w_β is indeed a homomorphic expansion of $\widetilde{wTF}$: in other words, we need to show that V_β and C_β satisfy the equations (R4), (U), and (C) of Fact 2.5. Unfortunately, doing this directly seems difficult.

Note that (R4), which is in some sense the "main equation", is an equality between different circuit algebra – in fact, planar algebra – compositions of crossings. Hence, the proof would be much easier if Z^u were to be a circuit algebra – or planar algebra – map. This unfortunately makes no sense, as *sKTG* is not a circuit or planar algebra but a different, more complicated algebraic structure. The reader might ask, why work with a space as inconvenient as *sKTG* instead of, say, a planar algebra of trivalent tangles? The answer is that the existence of a homomorphic expansion is a highly non-trivial property, and in particular ordinary trivalent tangles do not have one. Even without trivalent vertices, ordinary tangles, or u-tangles, do not have have a homomorphic expansion as a planar algebra[10]. *Parenthesized tangles* (a.k.a. *q-tangles*) [LM, BN2] do have homomorphic expansions, yet in fact these are almost equivalent to *sKTG* [T, BND1, Da].

[10]We only mention that the planar algebra of u-tangles does not have a homomorphic expansion Z^t so as to explain why we are not using one. This said, the non-existance of Z^t is easy to prove: by an explicit calculation in degree 2 one shows that there is no linear combination of chord diagrams that can serve as $Z^t(\times)$, which satisfies the R3 relation.

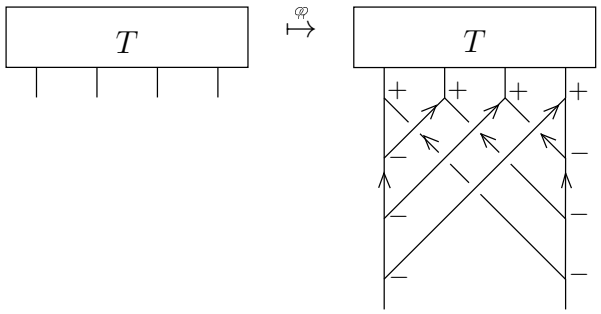

Figure 16. The *double tree map*: connect the ends of T by two binary trees (hence "double tree"), as shown. Note that the tree on the left always crosses over the tree on the right, and all edges of both trees are oriented towards T.

fig:dt

Nonetheless, we put planar algebras to use in a less direct way to prove the R4 equation: we map ordinary trivalent tangles into *sKTG* via a *double tree* construction, and use this to define Z^w for the a-images of all usual trivalent tangles. Then we use the planar algebra structure to prove that this Z^w is a homomorphic expansion (that is, satisfies the (R4), (U) and (C) equations), and finally show that the Z^w constructed this way is in fact the same as the one arising from part (1).

eq:R4 eq:U eq:C

bsec:ZwDef

3.3.1. *Defining Z^w.* We start by defining (classical, or *usual*) trivalent tangles, denoted $u\mathcal{T}T$:

$$u\mathcal{T}T := \mathrm{PA}\left\langle \; \diagup\!\diagdown,\ \diagdown\!\diagup,\ \uparrow\!\diagdown,\ \diagup\!\downarrow \;\middle|\; \mathrm{R1}^s,\ \mathrm{R2},\ \mathrm{R3},\ \mathrm{R4} \;\middle|\; S_e,\ u_e \right\rangle$$

Here PA stands for *planar algebra*: an algebra over the operad of planar tangles, that is, an algebraic structure similar to a circuit algebra, except with *planar* wiring diagrams. (See [DHR1, Section 3.1] for a detailed definition. This is a slightly more simple-minded notion than the original use of the term in [J], in particular we do not use checkerboard shadings.)

DHR:IsrcAlg jones:PlanarAlgebras

The elements of $u\mathcal{T}T$ are usual – that is, classical – trivalent tangles with ordered ends (the ordering is assumed to be counterclockwise from bottom left, unless otherwise stated), and signed vertices with a total ordering of edges at each vertex. There are no "virtual crossings" in planar algebras. The relations are the usual Reidemeister relations which make sense in this context ($\mathrm{R1}^s$, R2, R3 and R4). The planar algebra $u\mathcal{T}T$ is equipped with auxiliary orientation switch and edge unzip operations. Edge unzips are defined for edges that connect a positive and a negative vertex in as shown in the figure on the right. The planar algebra $u\mathcal{T}T$ does not have a homomorphic expansion.

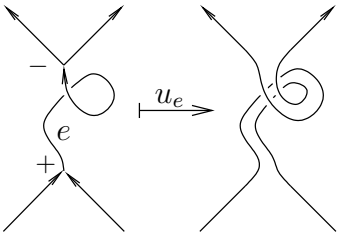

We define a *double tree* map $\wp : u\mathcal{T}T \to sKTG$, as in Figure 16. The map $\wp$ depends on two choices of binary trees: in Figure 16 we chose a particular example. It is important that, regardless of the choice of trees, the "left side" tree crosses over the "right side" tree. We will demonstrate that in fact the choice of trees becomes irrelevant after some post-compositions, see Lemma 3.3.

fig:dt fig:dt lem:TreeChange

Working towards a construction of Z^w, we post-compose $\wp$ with the following sequence of maps, which are explained in the paragraph below:

$$T \in u\mathcal{T}T \xrightarrow{\wp} sKTG \xrightarrow{Z^u} \mathcal{A}^u(\wp(T)) \xrightarrow{\alpha} \mathcal{A}^{sw}(\wp(T)) \xrightarrow{\kappa,u,p} \mathcal{A}^{sw}(\check{T}) \overset{\varphi}{\cong} \mathcal{A}^{sw}(T). \tag{5}$$

eq:dt

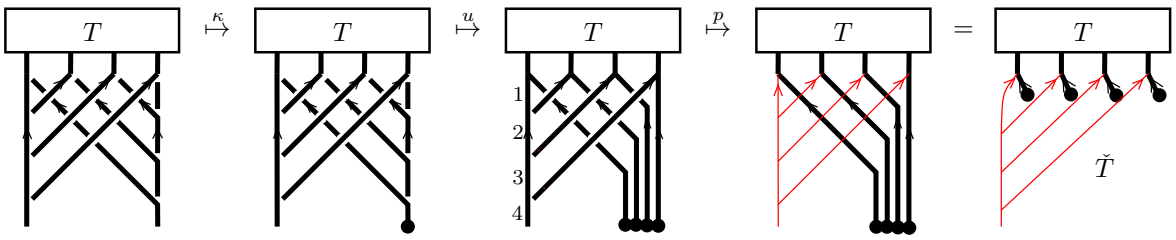

Figure 17. The cap attachment, unzips and punctures. While these operations are applied in $\mathcal{A}^{sw}$ – there are arrows on these skeleta – for simplicity the figure only shows the effect on the skeleton.

fig:pCu

Here T stands for an arbitrary tangle in uTT. The double tree map sends T into $sKTG$, and by applying Z^u one obtains a value in $\mathcal{A}^u$, namely a chord diagram on the skeleton of $\wp(T)$. We denote the space of chord diagrams on this skeleton by $\mathcal{A}^u(\wp(T))$. Now α maps this to arrow diagrams on the skeleton of $\wp(T)$, that is, to $\mathcal{A}^{sw}(\wp(T))$. In order to revert the skeleton back to that of T, we apply some operations in $\mathcal{A}^{sw}$: a cap attachment κ, unzips and punctures (as shown in Figure 17 and explained below), resulting in a slightly modified version of the desired skeleton, denoted $\check{T}$. Finally, we use that $\mathcal{A}^{sw}(\check{T}) \cong \mathcal{A}^{sw}(T)$ via the sorting isomorphism φ of Lemma 2.4, and hence we obtain a value in $\mathcal{A}^{sw}(T)$, as needed, which, we will later see, is *almost* $Z^w(a(T))$. (Although the punctured strands connect in a single binary tree, VI relations can be used as part of the sorting isomorphism.)

fig:pCu

lem:CapString

The cap attachment, unzip and puncture operations are done in the order shown in Figure 17. First attach a cap – a capped strand with no arrows on it – to the end of the right vertical strand in $\alpha(\wp(T))$: this is a circuit algebra operation in $\mathcal{A}^{sw}$. If T has n ends, perform $(n-1)$ consecutive disc unzips on the capped strand, as shown in Figure 17. Then puncture the left hand tree, for example by puncturing the left vertical strands marked "1, 2,..." in Figure 17 (these punctures also affect the connecting diagonal strands, as in Figure 5). Note that since the punctured tree had originally crossed over the capped tree, these crossings become virtual after puncturing, hence the last equality in Figure 17.

fig:pCu

fig:pCu

fig:punctures

fig:pCu

eq:dt

Denote the composition of the maps and operations shown in Equation (5) by ξ, that is,

$$\xi := \varphi \circ p \circ u \circ \kappa \circ \alpha \circ Z^u \circ \wp. \tag{6}$$

eq:xidef

Then, $\xi(T) \in \mathcal{A}^{sw}(T)$. We first show that $\xi(T)$ is well-defined, that is, it doesn't depend on the choice of binary trees in $\wp(T)$.

TreeChange

Lemma 3.3. *The choice of binary trees in the double tree construction does not affect* $\xi(T)$.

Proof. Any binary tree can be changed into any other binary tree via a sequence of "I to H" moves, as shown on the right. Hence, it is enough to analyze how an I to H move on one of the trees affects the value of $Z^u(\wp(T))$, and prove that the difference vanishes after the caping, unzip, and puncture operations.

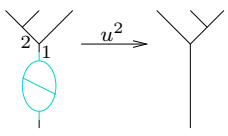

Suppose τ_1 and τ_2 are two binary trees which differ by a single I to H move, and let $\wp_{\tau_1}$ and $\wp_{\tau_2}$ denote the two resulting double-tree maps, assuming the "other side tree" is unchanged. The I to H move can be realised by inserting[11] an associator, followed by unzipping the edge marked '1' on

Bar-NatanDancso:WKO2

[11] See [WKO2, Section 4.6] for a detailed description of the tangle insertion operation in *sKTG*.

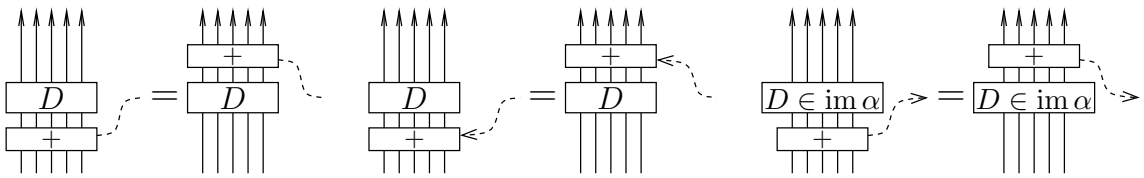

Figure 18. The invariance property of chord diagrams on the left, the head invariance and tail invariance properties of arrow diagrams in the middle and right. Here D denotes a chord or arrow diagram on any skeleton; for tail invariance there is a restriction that $D \in \operatorname{im}\alpha$ (with $\alpha : \mathcal{A}^u \to \mathcal{A}^{sw}$). The box labelled "+" denotes a sum of incoming chords or arrows, whose other ends are in the same place. The equalities are understood locally: there may be other skeleton components and chords/arrows elsewhere, which coincide on both sides. fig:Invari

the right, then the edge marked '2'. By the homomorphicity of Z^u, the values $Z^u(\wp_{\tau_2}(T))$ and $Z^u(\wp_{\tau_1}(T))$, only differ in an inserted horizontal chord associator Φ on the three strands involved, we indicate this by writing $Z^u(\wp_{\tau_2}(T)) = Z^u(\wp_{\tau_1}(T)) * \Phi$. If the I to H move was done on the left side tree, then all the strands involved are later punctured, killing any arrow diagram that lived on them by the TF relation. As a result, the only surviving part of Φ is its constant term, 1, and the resulting values of ξ are equal.

If the I to H move is done on the right side tree, then the all participating strands are capped and disk unzipped. If $\alpha(\Phi)$ is immediately adjacent to the caps, then it cancels by the CP relation. However, it is a priori possible that there are other arrow ending separating Φ from the caps. Note that in $\mathcal{A}^u$, any chord endings can be can be commuted from below the associator to above, using VI relations and the *invariance property* of chord diagrams shown in Figure 18 [BN2, Lemma 3.4]. Thus, one can assume that $\alpha(\Phi)$ is adjacent to the caps and hence cancels. This concludes the proof. □

There is an action of $\mathbb{Z}/n\mathbb{Z}$ on elements of $\mathcal{UTT}$ with n ends, by cyclic permutations of the ends. The following lemma will be useful later in proving that Z^w is a planar algebra map; we present it now because its proof is similar to that of Lemma 3.3. lem:freeChange

CyclicPerm **Lemma 3.4.** *The map ξ is invariant under cyclic permutation of the ends of T.*

Proof. To show that $\xi(T)$ is invariat under cyclic permutations of ends of T, it is enough to show that $\xi(T)$ does not change when the rightmost end of T is moved to the far left (denote this by σT), as shown in Figure 19. fig:welldef

The rightmost picture of Figure 19 is equivalent as *sKTG*s to $\wp(\sigma T)$. It differs from $\wp(T)$ in three ways:

- the binary trees connecting the ends of T are different;
- two tree branches (marked with $*$ in Figure 19) are connected to the trunk from the opposite side: that is, these trivalent vertices have opposite cyclic orientation;
- one tree branch has a kink in it.

As before, we need to analyse how $Z^u(\wp(\sigma T))$ differs from $Z^u(\wp(T))$, and show that the difference vanishes after the puncture, cap and unzip operations.

To achieve this, we transform $\wp(\sigma T)$ into $\wp(T)$ using tangle insertions. First, cancel the kink by inserting an opposite kink I_1 on the same strand, as shown in Figure 20 in blue[12]. fig:welldef2

[12]Or grey in black and white print.

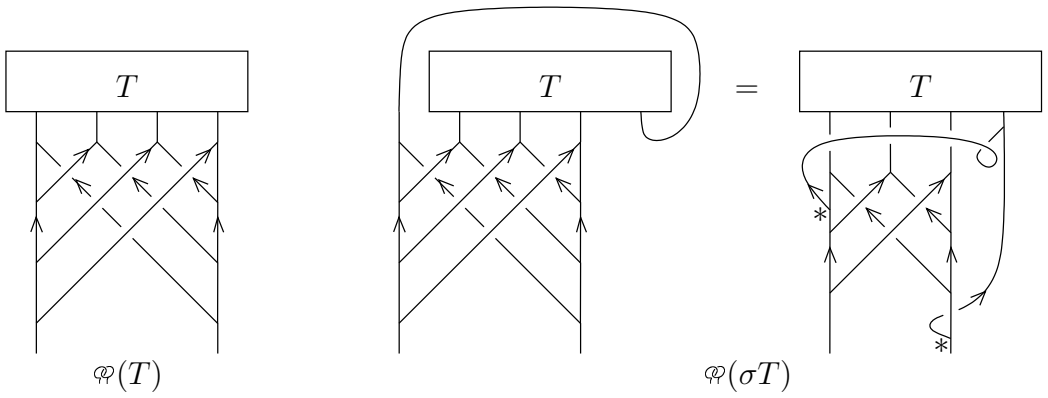

Figure 19. Double tree construction for cyclically permuted ends of T.

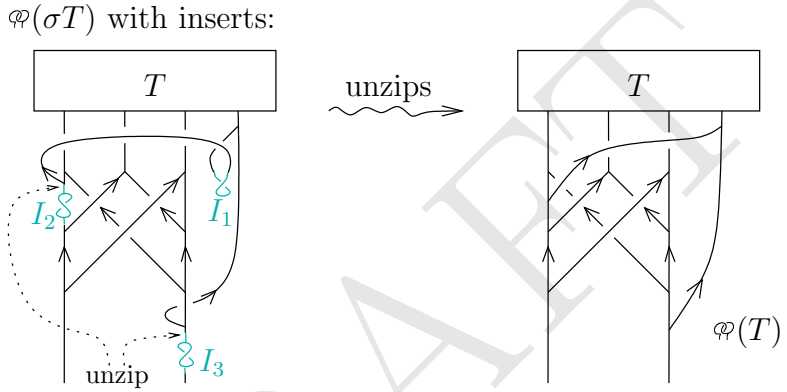

Figure 20. The difference between $\wp(T)$ and $\wp(\sigma T)$, understood via insertions.

As Z^u is compatible with insertion, the Z^u values will differ by the value of a kink: a chord diagram on the one strand involved. Later in the process this strand is punctured, so the value of the kink cancels by the TF relation.

Similarly, switching the side that the tree branches are attached on amounts to inserting twists I_2 and I_3, and unzipping the connecting edges, also shown in Figure 20. Each of these operations changes the value of Z^u by inserting the value of a twist, which is $e^{c/2}$ for any Z^u, where c denotes a single chord between the appropriate strands [WKO2, Lemma 4.14]. Applying α maps this to $e^{(a_L+a_R)/2}$, where a_L and a_R denote horizontal left and right arrows, respectively. On the left side tree, this cancels after punctures, as before. On the right side tree, the strand directly underneath the twist is capped and uzipped, and hence the value of the twist cancels by the CP relation.

Now observe that the right side picture of Figure 20 only differs from $\wp(T)$ in the choices of binary trees, which do not change the value of ξ by Lemma 3.3. □

The following lemma clarifies the relationship between the map ξ and the homomorphic expansion Z^w that we're aiming to construct:

Lemma 3.5. *If there exists a homomorphic expansion Z^w for $\widetilde{wTF}$ compatible with Z^u, and $T \in uTT$ is a tangle with n ends, then $Z^w(a(T)) = \xi(T) \cdot (C^{-1})^n$, where $C = Z(\downarrow)$, and $\xi(T)$ is multiplied by C^{-1} at each tangle end of T, as in Figure 22.*

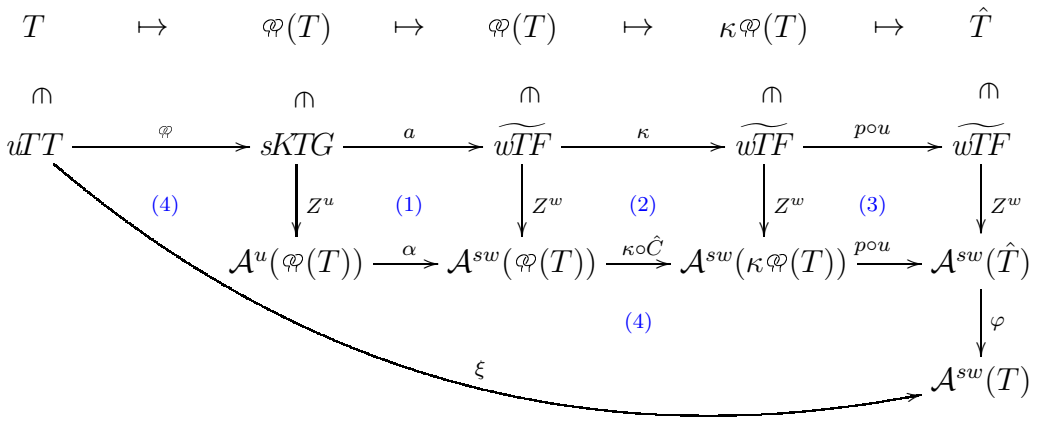

Figure 21. Comparing ξ and Z^w, assuming that Z^w exists. fig:BigCom

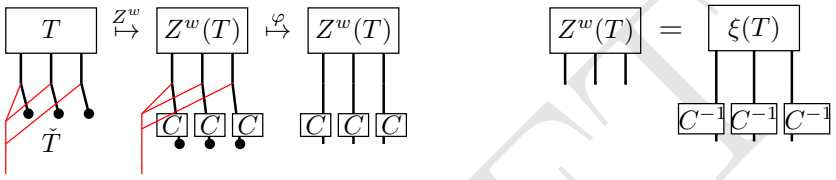

Figure 22. Computing $Z^w(\check{T})$ and $Z^w(T)$. fig:ZTChec

Proof. Assume there exists a homomorphic expansion Z^w compatible with Z^u. We use, as in Figure 21, the homomorphicity of Z^w and its compatibility with Z^u to show that $\xi(T) = Z^w(\check{T})$, where $\check{T}$ is as in Equation 5 and shown in Figure 22 on the left.

If the diagram in Figure 21 commutes, then for any $T \in \mathit{wTT}$ and any Z^u-compatible Z^w, we have $\varphi(Z^w(\check{T})) = \xi(T)$. Since Z^w is a circuit algebra homomorphism, $Z^w(\check{T})$ can be obtained from $Z^w(T)$ by attaching the Z^w-value of a left-punctured right-capped vertex at each tangle end, as illustrated in Figure 22. By Lemma 2.8 we have $Z^w\left(\right) = 1$, so the only additions are C values at each capped end, as shown in Figure 22. This can then be interpreted as a value in $\mathcal{A}^{sw}(T)$ via the isomorphism φ of Lemma 2.4. This implies the statement of the Lemma.

It remains to show that the diagram in Figure 21 commutes. The square (1) is the assumed the compatibility of Z^u and Z^w. In square (2), recall the map κ denotes the circuit algebra operation of attaching a cap at the bottom right end of the w-foam. The map $\hat{C}$ denotes the circuit algebra operation which attaches a value $C = Z(\downarrow)$ at the end of the strand. Thus, the commutativity of square (2) is implied by the homomorphicity of Z^w with respect to circuit algebra composition (as a binary operation). The square (3) is commutative due to the homomorphicity of Z^w with respect to punctures and disc unzips.

The commutativity of the heptagon (4) would be true by definition, if not for the map $\hat{C}$ (multiplication by the cap value). We show that, in fact, the value C cancels after punctures, by a property of arrow diagrams in the image of α, called *tail-invariance*, shown in Figure 18 (see [WKO2], Remark 3.14 and early in Section 3.3). In the current situation tail invariance means that the value C, which has only arrow tails, can be moved from one tangle end to the other, as shown on the right. Consequently, C cancels when the left strand is punctured. □

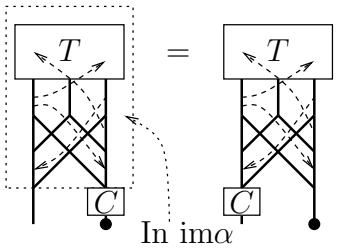

Remark 3.6. In Lemma 3.5 we assume by convention that all tangle ends of T are oriented upwards (towards T). If k tangle ends are oriented down, the corresponding cap values appear with their orientations switched: $Z^w(aT) = \xi(T) \cdot (C^{-1})^{n-k}(S(C)^{-1})^k$.

Corollary 3.7. *If there exists a homomorphic expansion Z^w for $\widetilde{wTF}$ compatible with Z^u, then $\pi(V) = \pi(\xi(\curlywedge))$, where V is the Z^w-value of the vertex, and π is the tree projection. This uniquely determines Z^w.*

Proof. The first statement is an immediate consequence of Lemma 3.5. The second was shown in Section 3.1.2. □

Thus, the map ξ uniquely determines Z^w, assuming that Z^w exists: from here on we denote this candidate homomorphic expansion by Z^w_ξ. We have shown how to explicitly compute $\pi(V)$ from Z^b through ξ. What remains to be proven is that:

(1) Z^w_ξ is compatible with Z^u: see Proposition 3.10 below.
(2) The restriction of Z^w_ξ to $a(\widetilde{wTT})$ is a planar algebra map (see Theorem 3.13 below), and thus Z^w_ξ satisfies the (R4) equation.
(3) Z^w_ξ satisfies the (U) and (C) equations, hence it is a homomorphic expansion of $\widetilde{wTF}$ compatible with Z^u: see Theorem 3.18 below.
(4) The expansion Z^w_ξ is the same as Z^w_β obtained from the "buckle" construction of Section 3.1.1: $V = Z^w\xi(\curlywedge) = V_\beta$ and $C = Z^w_\xi(\bullet) = C_\beta$. This is done in Lemma 3.15 below.
(5) Thus, there exists a unique homomorphic expansion $Z^w = Z^w_\xi = Z^w_\beta$, compatible with Z^u, see Proposition 3.18 below.

While the construction of Z^w_ξ enables us to prove the (R4) and (U) equations, Z^w_β is computationally simpler, and thus we use step (4) and C_β to prove that the (C) equation is satisfied.

3.3.2. *Z^w_ξ is a homomorphic expansion.* The goal for this subsection is to complete the sketch above. We begin by showing that Z^w_ξ is compatible with Z^u. This requires a technical lemma, in which we compute the ξ-value of a vertical strand:

Lemma 3.8. *For a single un-knotted strand, $\xi(\frown) = \alpha(\nu^{1/2})$, where $\nu \in \mathcal{A}^u(\frown)$ denotes the Kontsevich integral of the un-knot*[13].

Proof. We apply $\wp$ to $\frown$, as shown in Figure 23, and comupte $Z^u(\wp(\frown))$ using the finite generation property of *sKTG* and the homomorphicity of Z^u. In [WKO2, Section 5.2] we

[13] The value of ν was conjectured in [BGRT] and proven in [BLT]. Note that ν involves wheels only.

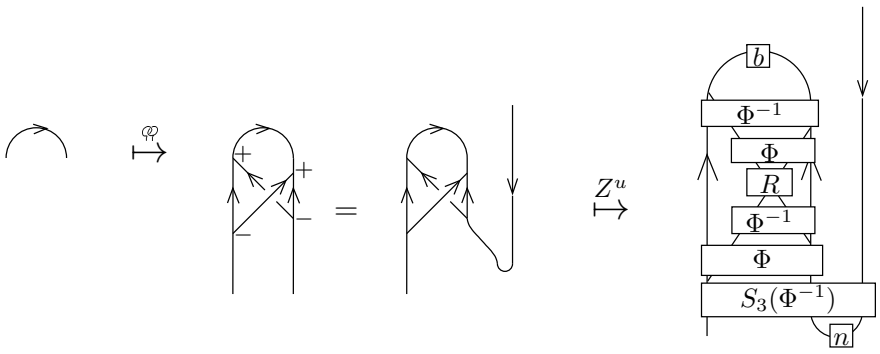

Figure 23. The double tree map composed with Z^u, applied to a single strand. To compute $Z^u(\wp(\curvearrowright))$, we write $\wp(\curvearrowright)$ as a composition of generators; this requires first expressing it as a bottom-top tangle. See [WKO2, Proposition 4.13] for details.

gave an algorithm for writing any *sKTG* as an *sKTG*-composition of generators (the primary operation in *sKTG* is *tangle insertion*, see [WKO2, Figure 22]). Feeding $\wp(\curvearrowright)$ into this algorithm, one needs to "curve up" one strand as in Figure 23, in this case the strand on the right (the choice of strand doesn't affect the outcome).

The chord diagram $Z^u(\wp(\curvearrowright))$ is shown in Figure 23, expressed in terms of the generators of *sKTG* described in [WKO2, Proposition 4.13]: the value Φ of the *associator graph*, which is a Drinfel'd associator; the value $R = e^{c/2}$ of the *twist graph*, where c is a single chord; and the values n and b of the *noose* and *balloon* graphs, respectively.

In $\xi(\curvearrowright)$, Z^u is followed by α, a cap attachment, unzips and punctures. As explained in [WKO2, Section 4.6], there is possibly a one-parameter freedom in the values of n and b, but we know that and $\alpha(b) = e^{a/2}\alpha(\nu)^{1/2}$, and $\alpha(n) = e^{-a/2}\alpha(\nu)^{1/2}$. The exponential part of n cancels by the CP relation once the cap is attached. The wheels part $\alpha(\nu)^{1/2}$ can be moved to the bottom left end by the tail invariance property (as in the last paragraph of the proof of Lemma 3.5), where it cancels after punctures. For the associator $S_3(\Phi^{-1})$ at the bottom in Figure 23, there is an orientation switch S_3 applied as the third strand is oriented downwards. In fact, $S_3(\Phi^{-1})$ cancels by Fact (2) of Lemma 3.2.

Taking these cancellations into account, the value $pu\kappa\alpha Z^u\wp(\curvearrowright) \in \mathcal{A}^{sw}$ is shown in Figure 24 and explained below. Recall that α maps a chord to the sum of its two possible orientations. However, when one supporting strand is punctured, only one of these orientations survive. Hence, for example, $p_2(\alpha(R_{23})) = (e^{a_{32}/2})$. Figure 24 shows a schematic picture of $pu\kappa\alpha Z^u\wp(\curvearrowright)$ with exponentials and associators indicated by single arrows. Recall that $\Phi \in \mathcal{A}^{hor}(\uparrow_3)$ can be written as a power series in any two of the three generators of $\mathcal{A}^{hor}(\uparrow_3)$: c_{12}, c_{23} and c_{13}. For example, $\Phi(c_{12}, c_{23}) = \Phi(c_{12}, -c_{12} - c_{23})$. For each associator we chose the presentation in which $pu\kappa\alpha(\Phi)$ is of the simplest form.

(1) The top associator of Figure 23, after applying a VI relation, is written as $\Phi^{-1}_{13(24)}$ in the strand numbering of Figure 24. We write this in terms of c_{13} and $c_{1(24)} = c_{12} + c_{14}$, since after the puctures $p_1\alpha(c_{13}) = a_{31}$ and $p_1p_2\alpha(c_{1(24)}) = a_{41}$, thus

$$p_1p_2\alpha\Phi^{-1}(c_{13}, -c_{13} - c_{1(24)}) = \Phi^{-1}(a_{31}, -a_{31} - a_{41}).$$

This is reflected in Figure 24 in drawing only the a_{31} and a_{41} arrows. In turn, the associator cancels, essentially by Fact (2) of Lemma 3.2: strand 5 acts as a

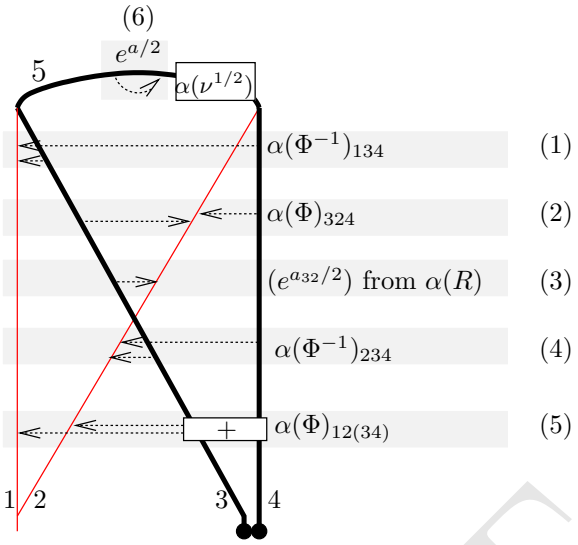

Figure 24. The value of $pu\kappa\alpha Z^u\wp(\curvearrowright)$: the numbering (1) through (6) refer to the paragraphs where each component is explained.

fig:dtstra

concatenation of strands 3 and 4, as the tail of a_{41} can be "pulled over the top along strand 5" using the VI relations and the fact that $e^{a/2}\alpha(\nu)$ is a local arrow diagram on a single strand, hence it is central. Thus, $a_{41} = a_{31}$, and $\Phi^{-1}(a_{31}, -a_{31} - a_{41}) = \Phi^{-1}(a_{31}, -2a_{31}) = 1$ as the arguments commute. Therefore

$$p_1p_2\alpha(\Phi^{-1}_{13(24)}) = 1.$$

(2) Second from top we have

$$p_1p_2\alpha(\Phi_{324}) = p_1p_2\alpha(\Phi(c_{23}, c_{24})) = \Phi(a_{32}, a_{42}) = 1,$$

by the same modified version of Fact (2) (concatenation).

(3) For the exponential,

$$p_1p_2\alpha(R_{23}) = p_1p_2\alpha(e^{c_{23}/2}) = e^{a_{32}/2}.$$

(4) Next,

$$p_1p_2\alpha(\Phi^{-1}_{234}) = p_1p_2\alpha(\Phi^{-1}(c_{23}, -c_{23} - c_{24})) = \Phi(a_{32}, -a_{32} - a_{42}) = 1$$

by the modified Fact 2, noting that the arrow tails also commute with the arrow tails of the exponential.

(5) By Fact (1)

$$p_1p_2\alpha(\Phi)_{12(34)} = 1.$$

(6) Finally, move the top exponential $e^{a/2}$ to strands 3 and 2, using the VI relation at both vertices. The tail of each arrow moves freely from strand 5 to strand 3. The heads commute with $\alpha(\nu)$, they are killed on strand 4 due to the CP relation, so they slide onto strand 2 but acquire a negative sign due to opposite orientations. Hence, $(e^{a_{55}/2}) = (e^{-a_{32}/2})$, and this cancels $\alpha(R)$. In summary, $\xi(\curvearrowright) = \alpha(\nu^{1/2})$, as claimed.

□

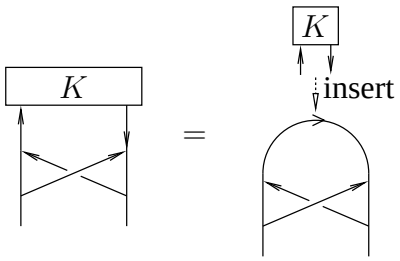

Figure 25. For $K \in sKTG$, $\wp(K)$ is K inserted into $\wp(\uparrow)$.

As an aside, Lemma 3.8 enables a quick computation of the even part of $C = e^c = Z^w_\xi(\,\downarrow)$. Recall that c is a linear combination of wheels: $c = \sum_{n=2}^{\infty} \gamma_n w_n$. Let $c = c_0 + c_1$, where c_0 denotes the even part of c (sum of all even wheels), and c_1 denotes the odd part, that is, $c = c_0 + c_1$. Let $C_0 = e^{c_0}$, the even part of C. Corollary 3.9 shows in particular that the even part of the C is independent of the choice of Z^b (that is, the choice of Drinfel'd associator) and Z^u.

Corollary 3.9. *If $C = Z^w_\xi(\,\downarrow)$, and C_0 is the even part of C, then $C_0 = \alpha(\nu^{1/4})$, regardless of the choice of expansion Z^u used to construct Z^w_ξ.*

Proof. By Lemma 3.5 and Remark 3.6, we have $Z^w_\xi(\uparrow) = C^{-1}\xi(\uparrow)S(C^{-1})$: see the figure on the right for the orientations. Note that $S(w_{2k}) = w_{2k}$ and $S(w_{2k+1}) = -w_{2k+1}$, and hence $S(C) = e^{c_0 - c_1}$. Also, by homomorphicity, $Z^w_\xi(\uparrow) = 1$. Thus, by Lemma 3.8, $1 = e^{c_0+c_1}\alpha(\nu^{1/2})e^{c_0-c_1}$, and therefore $\alpha(\nu^{1/2}) = e^{2c_0}$, which gives $C_0 = e^{c_0} = \alpha(\nu^{1/4})$. □

Next we prove that Z^w_ξ is indeed compatible with Z^u:

Proposition 3.10. *For any $K \in sKTG$, $Z^w_\xi(a(K)) = \alpha(Z^u(K))$.*

Proof. Note that $sKTG \subseteq \mathcal{uTT}$, and for $K \in sKTG$, $\wp(K)$ can be obtained by inserting K into the top strand of $\wp(\uparrow)$: see Figure 25. Since Z^u is compatible with insertions, $Z^u(\wp(K))$ can be obtained by $Z^u(K)$ inserted into $Z^u(\wp(\uparrow))$. Through the sequence of α, capping, puncturing, φ and multiplications by C^{-1}, all of $Z^u(\wp(\uparrow))$ cancels, as in Lemma 3.8. Note that the cancellations still go through despite the fact that $\alpha(Z^u(K))$ is inserted on the top strand: this follows from the fact that $\alpha(Z^u(K))$ is in the α-image of $\mathcal{A}^u$, and the appropriate "commutativity" property holds in $\mathcal{A}^u$. Hence, $Z^w_\xi(K) = Z^w_\xi(K)$ as required. □

Now, we show that Z^w_ξ it is a planar algebra homomorphism on $a(\mathcal{uTT})$. This is technically challenging, but it implies the R4 equation immediately. For the proof, it will be necessary to know the behaviour of Z^u with respect to edge deletions. When an edge e of a knotted trivalent graph $K \in sKTG$ is deleted, the two vertices at each end of e cease to be vertices. The associated graded operation on chord diagrams deletes skeleton edge e, and chord diagrams with any chord endings on e are set equal to 0.

Fact 3.11. *Z^u commutes with edge deletions up to a possible correction term of $e^{\pm c/4}\nu^{1/2}$ depending on the position of the edge, as in Figure 26.*

Proof sketch. In [WKO2, Section 4.6.1] Z^u is constructed from an invariant Z^{old} by adding vertex normalizations, as shown in Figure 26. Note that the top two diagrams in figure

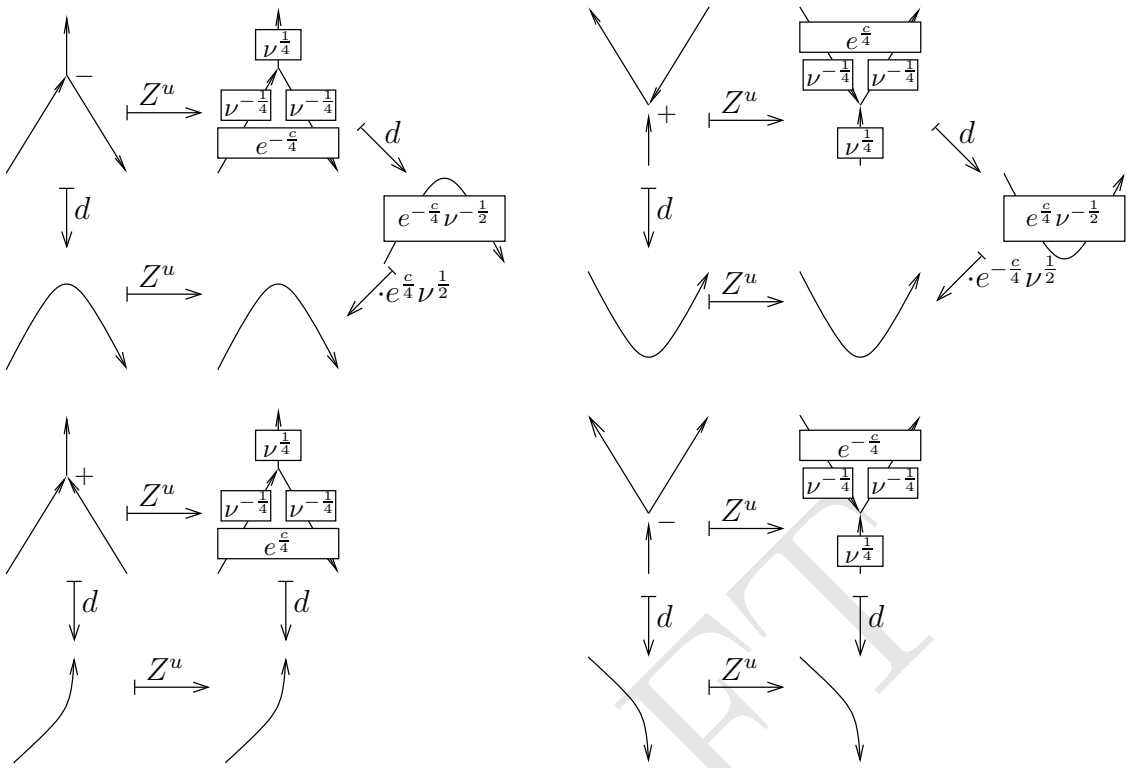

Figure 26. In [WKO2, Section 4.6.1] Z^u is constructed from an invariant Z^{old} by applying vertex normalizations, which depend on vertex signs: these are shown along the top horizontal arrow of each diagram (see also [WKO2, Figure 29]). It follows Z^u is only homomorphic up to a correction term when deleting the top edge of a positive vertex (first in the total ordering around the vertex) or the bottom edge of a negative vertex: see the top two diagrams. In other edge deletions the normalizations cancel, and hence Z^u is homomorphic with respect to these edge deletions, as for example in the bottom two diagrams.

differ from [WKO2, Figure 29] in a single edge orientation switch, which switches the vertex sign and accordingly the normalization[14]. In fact, Z^{old} commutes with edge deletions [Da, Proposition 6.7], so the edge deletion error (and hence, the correction term) for Z^u arises from the vertex normalisations implemented, as shown in Figure 26. □

Remark 3.12. There is also an "edge delete" operation of $\widetilde{wTF}$: this is not required for the finite presentation of $\widetilde{wTF}$ or $\mathcal{A}^{sw}$, but it is necessary for the proof of Theorem 3.13. When deleting an edge in $\widetilde{wTF}$ – which can be either a tube or a string – the vertices at either end[15] cease being vertices. The associated graded operation $d_e : \mathcal{A}^{sw} \to \mathcal{A}^{sw}$ deletes the skeleton edge e and sends any arrow diagram with arrow endings on the deleted strand to zero. The crucial fact we need is that edge delete operations for chord and arrow diagrams

[14]The point of the normalization is to make Z^u commute with unzips. The reader might wonder, why normalize so that the expansion respects unzips, rather than deletions? The answer is that for finite generation of knotted trivalent graphs, unzips are crucial but deletions are not.

[15]It is also possible to delete a capped edge.

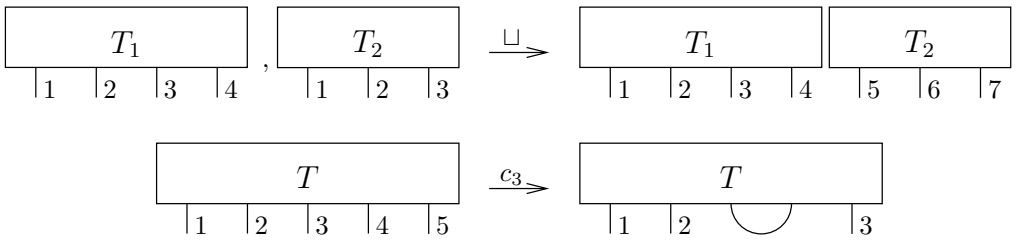

Figure 27. Basic planar algebra operations: disjoint union and contraction. fig:Atomic

are compatible via the map α, which is immediate from the definitions:

$$\begin{array}{ccc} \mathcal{A}^u & \xrightarrow{\alpha} & \mathcal{A}^{sw} \\ \downarrow{\scriptstyle d_e} & & \downarrow{\scriptstyle d_e} \\ \mathcal{A}^u & \xrightarrow{\alpha} & \mathcal{A}^{sw} \end{array}$$

thm:PAMap **Theorem 3.13.** *The restriction of Z^w_ξ to $a(\mathcal{UTT})$ is a planar algebra map.*

Proof. Planar algebra operations can be written as compositions of two simpler, basic operations: disjoint unions and contractions. In the disjoint union of two tangles T_1 and T_2, the ends of $T_1 \sqcup T_2$ are ordered by declaring that the ordered ends of T_1 come first, followed by the ordered ends of T_2. The contraction operation c_i applies to any tangle with at least $i+1$ ends: it acts by joining the i-th and $(i+1)$-st ends of T and re-numbering the rest, resulting in a tangle with two less ends. Both operations are shown in Figure 27. fig:AtomicPAOps

Thus, we only need to show that Z^w_ξ commutes with these two operations, that is, $Z^w_\xi(T_1 \sqcup T_2) = Z^w_\xi(T_1) \sqcup Z^w_\xi(T_2)$, and $Z^w_\xi(c_i(T)) = c_i(Z^w_\xi(T))$. Note that the right sides of these equalities make sense: arrow diagrams on the skeleta of $a(\mathcal{UTT})$, where Z^w_ξ takes values, also form a planar algebra, and in particular disjoint union and concatenation of arrow diagrams is well defined.

Disjoint unions. We need to compute $\xi(T_1 \sqcup T_2)$, where $T_1, T_2 \in \mathcal{UTT}$. The value $\wp(T_1 \sqcup T_2)$ is shown in Figure 28. The binary trees in $\wp$ can be chosen arbitrarily by Lemma 3.3: Figure 28 shows the most convenient trees for this proof. fig:DisjUni lem:FreeChange:DisjUni

Observe that $\wp(T_1 \sqcup T_2)$ can be obtained as an *sKTG* by inserting $\wp(T_1)$ and $\wp(T_2)$ into a simpler *sKTG*, denoted H, as shown in the same figure (up to orientation switches which don't impact what follows and will be ignored). Hence, $Z^u(\wp(T_1 \sqcup T_2))$ is given by inserting $Z^u(\wp(T_1))$ and $Z^u(\wp(T_2))$ into $Z^u(H)$.

One could compute $Z^u(H)$ explicitly using the same algorithm as before, but we can avoid this work, as follows. All chords in $Z^u(H)$ can be assumed to be located in the rectangle shown in Figure 28 (using VI relations, if necessary). During the computation of ξ both supporting strands are punctured, and therefore $p^2\alpha(Z^u(H)) = 1$. This implies that $\xi(T_1 \sqcup T_2) = \xi(T_1) \sqcup \xi(T_2)$, and it follows via Lemma 3.5 that $Z^w_\xi(T_1 \sqcup T_2) = Z^w_\xi(T_1) \sqcup Z^w_\xi(T_2)$. fig:DisjUni lem:Compatibility

Contractions. Proving that Z^w_ξ commutes with contractions is more involved. By Lemma 3.4, we can assume that the ends contracted are the last (rightmost) two ends of the n ends of T. Hence we will drop the subscript from c_i and denote this operation simply by c. lem:CyclicPerm

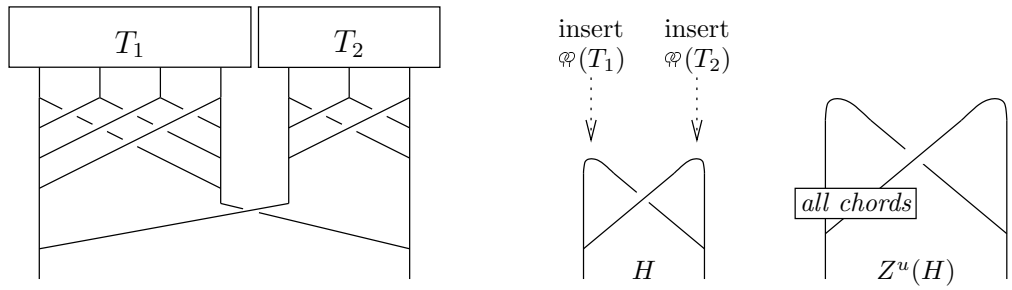

Figure 28. The double tree map applied to a disjoint union of $u\mathcal{TT}$-s is the same as inserting the double tree of each individual $u\mathcal{TT}$ into the *sKTG* H. In $Z^u(H)$ all chords can be pushed into the rectangle shown, using VI relations when necessary.

fig:DisjUn

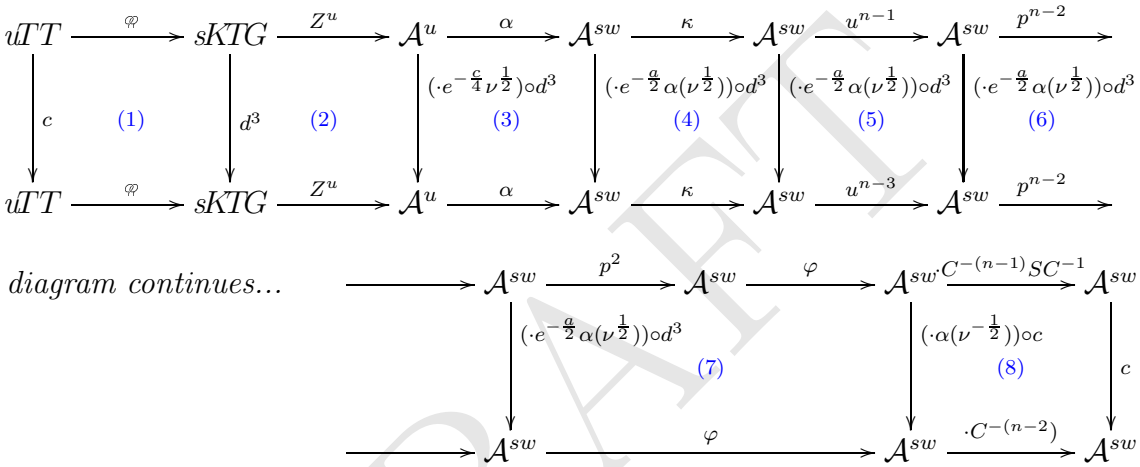

Figure 29. Summary of the proof that Z^w_ξ commutes with contractions: Z^w_ξ is the composition along the entire top and entire bottom horizontal edge of the diagram.

fig:Contra

We need to show that $Z^w_\xi(cT) = cZ^w_\xi(T)$, for any $T \in u\mathcal{TT}$. Since Z^w_ξ is given by the composition of many maps, so this can be restated as the commutativity of the perimeter of a large diagram (shown in Figure 29), which in turn can be broken down to its smaller parts. Throughout this proof, let $T \in u\mathcal{TT}$ denote an arbitrary trivalent tangle.

fig:ContractCommutes

Square (1). This square plays out in $u\mathcal{TT}$ and *sKTG*, and commutes by inspection, as shown on the right. The three strands to be deleted are indicated by broken lines. Therefore, $d^3\wp(T) = \wp c(T)$.

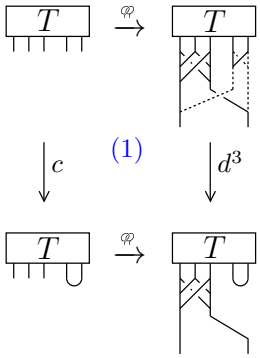

Square (2). Square (2) is shown schematically below on the left: for the Z^u-values skeleta are indicated but chords are not shown. To prove that square (2) commutes, we use the properties of Z^u with respect to deleting edges in *sKTG*, as stated in Fact 3.11 and Figure 26.

fact:ZuDelete fig:ZuDelete

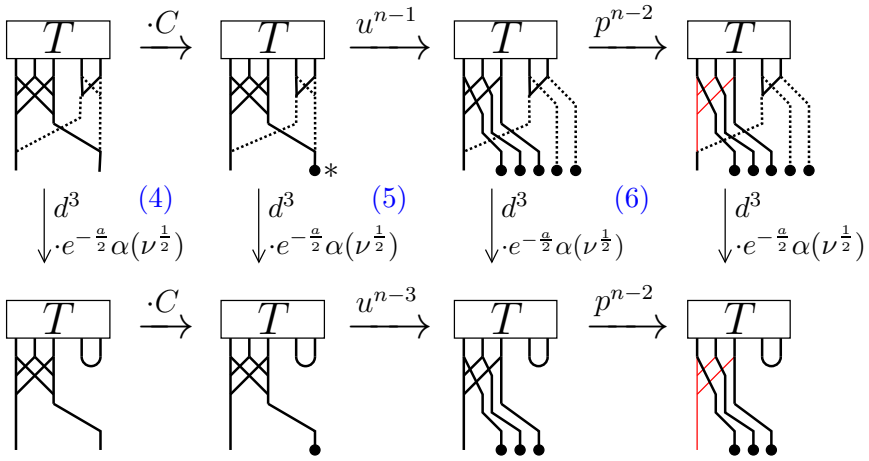

Figure 30. The squares (4) (5) and (6). Strands to be deleted are drawn in dashed lines throughout. The $*$ denotes a cap of interest: see the proof paragraph on square (5).

fig:456

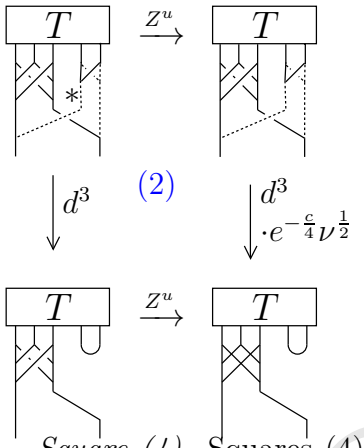

Only one of the three edge deletions requires a correction term: this is the edge marked with $*$ in the diagram on the left. This edge ends in a $e^{-c/4}\nu^{1/2}$ inserted at the place of the vertex, where c stands for a single chord. In square (2), this correction term appears at the bottom right corner of the square, where the two ends of T are contracted (see in the diagram showing skeleta in Figure 29). In summary: $\big(d^3 Z^u \wp(T)\big) \cdot (e^{-\frac{c}{4}}\nu^{\frac{1}{2}}) = Z^u \wp c(T)$.

fig:ContractCommutes

Square (3). Square (3) is essentially the commutativity of edge deletions stated in Remark 3.12, combined with applying α to the correction term. So we have:
$\big(d^3 \alpha Z^u \wp(T)\big) \cdot (e^{-\frac{a}{2}}\alpha(\nu^{\frac{1}{2}})) = \alpha Z^u \wp c(T)$.

rmk:wDelete

Square (4). Squares (4), (5), and (6) are shown in detail in Figure 30. Square (4) plays out in $\mathcal{A}^{sw}$ and it is commutative as the deletions and the cap attachments (denoted by κ) affect different strands: see the diagram on the right. Therefore,

fig:456

$$\big(d^3 \kappa\alpha Z^u \wp(T)\big) \cdot (e^{-\frac{a}{2}}\alpha(\nu^{\frac{1}{2}})) = \kappa\alpha Z^u \wp c(T).$$

Square (5). The only difference between $d^3 \circ u^{n-1}$ and $u^{n-3} \circ d^3$ is what happens to arrows on the caped skeleton edge marked by $*$ in Figure 30. Following the diagram right and down, this edge is unzipped $n-1$ times, then the last two of its daughter edges are deleted. On the other hand, following the diagram down and right, the same edge is unzipped $n-3$ times. The results of these compositions are the same by definition of the unzip and delete operations. Thus, we have

fig:456

$$\big(d^3 u^{n-1} \kappa\alpha Z^u \wp(T)\big) \cdot (e^{-\frac{a}{2}}\alpha(\nu^{\frac{1}{2}})) = u^{n-3} \kappa\alpha Z^u \wp c(T).$$

*Square (6).*The deletions and punctures occur on different strands, as shown in Figure 30, hence these operations commute commute. One detail to note is that when a tube strand is deleted at a "tube-and-string" vertex, all that is left is a string (as in the case of puncturing the tube at a tube-string vertex, see Figure 5). In summary:

fig:456

fig:punctures

$$\big(d^3 p^{n-2} u^{n-1} \kappa\alpha Z^u \wp(T)\big) \cdot (e^{-\frac{a}{2}}\alpha(\nu^{\frac{1}{2}})) = p^{n-2} u^{n-3} \kappa\alpha Z^u \wp c(T).$$

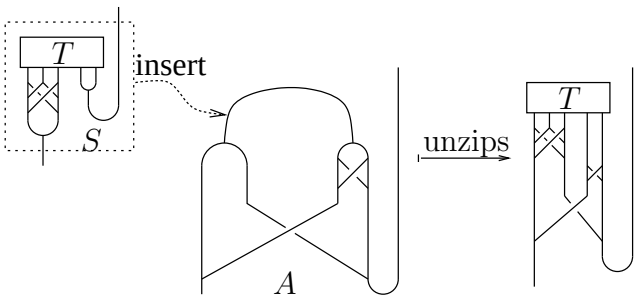

Figure 31. Computing the top left corner of Square 7, Step 1: $\varphi(T)$ can be expressed as the *sKTG* denoted S inserted into the *sKTG* denoted A, followed by unzips, as shown. Z^u respects insertions, hence computing $Z^u(A)$ determines the value of $Z^u(\varphi(T))$ outside of S.

fig:Square

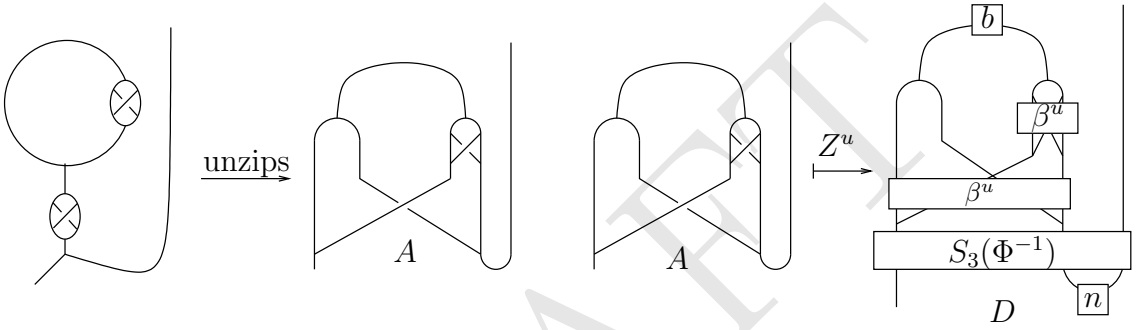

Figure 32. Computing the top left corner of Square 7, Step 2: computing $Z^u(A)$. The *sKTG* A can be obtained by inserting the *buckle sKTG* twice into a simpler *sKTG*, and unzipping, as shown on the left. The value of the buckle was computed in Figure 14. Using this value—denoted β^u—and the algorithm in [WKO2, Section 5.2], one computes $Z^u(A)$. The result is denoted D and shown on the right.

fig:BuckleBraid
Dar-NatanDancso:WKO2
fig:Square

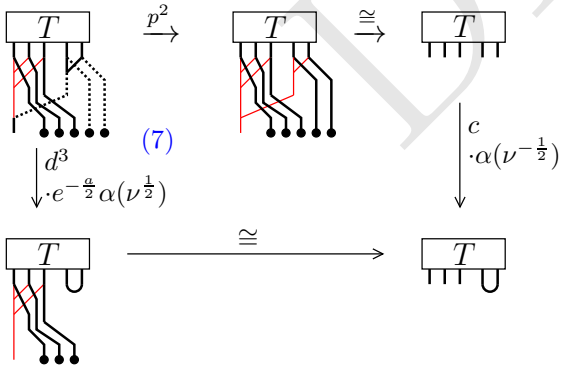

Pentagon (7). The pentagon (7) is shown on the left. This is the most delicate part of the proof. We first show that – for the specific input of $p^{n-2}u^{n-1}\kappa\alpha Z^u\varphi(T)$ – the pentagon (7) commutes up to a single possible error on the contracted (u-shaped) strand, and later prove that this error is necessarily zero.

To begin, a better understanding of the arrow diagram $p^{n-2}u^{n-1}\kappa\alpha Z^u\varphi(T)$ in the top left corner is necessary. All of the operations performed on T, with the exception of Z^u, are "easy" in the sense that we have a complete understanding of their effect. Z^u is "hard", but we can compute the relevant part of its value using the finite generation of *sKTG* ([WKO2, Proposition 4.13]). The computation is shown in Figures 31 and 32 and their captions.

Dar-NatanDancso:WKO2
fig:Square7Comm2
fig:Square7Comm2

In summary, $Z^u(\varphi(T))$ is given by inserting $Z^u(A)$ into the chord diagram D of Figure 32. Now we need to analyze what happens when one applies α, the cap attachment, unzips and punctures to this value: this is an exercise similar to what has been done for Lemma 3.8 for

lem:xiofstrand

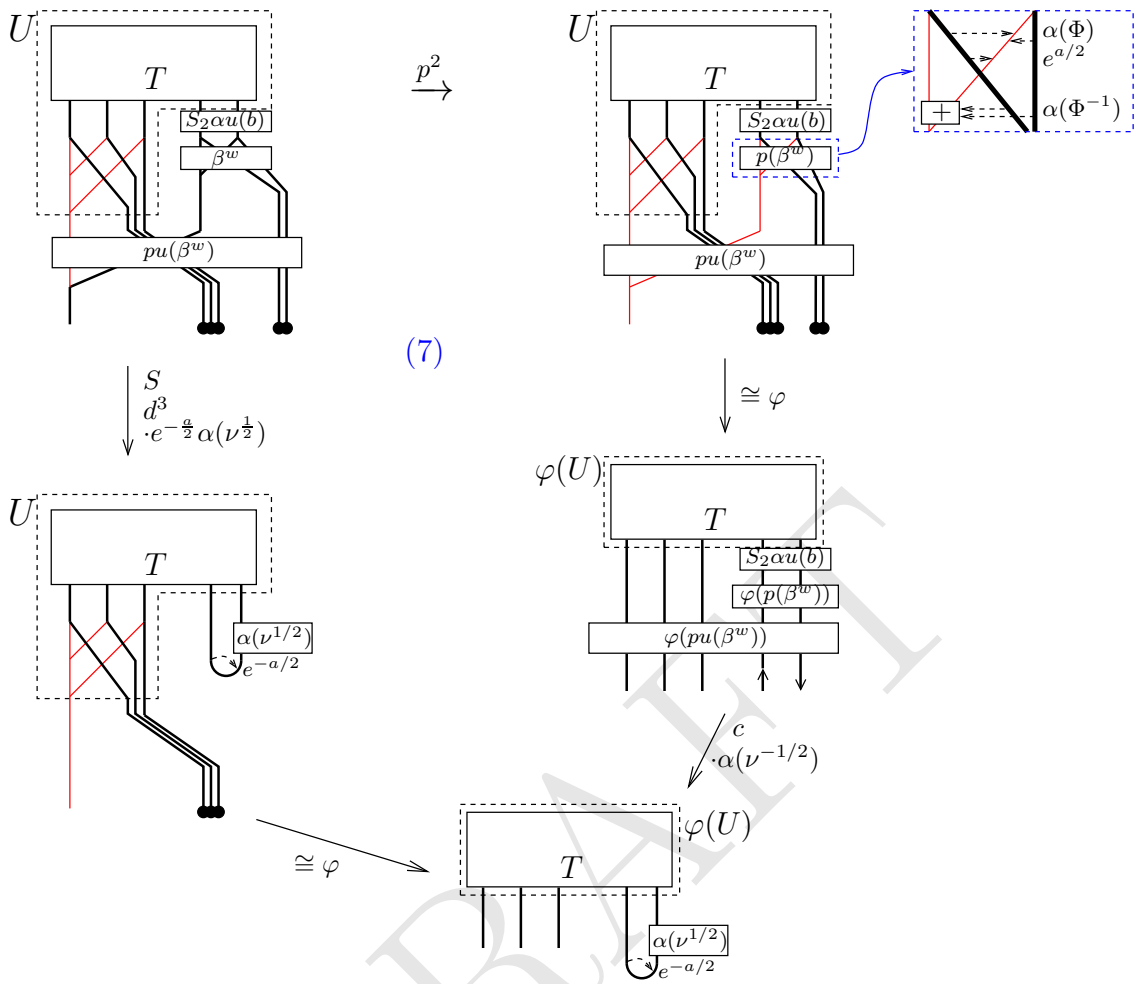

Figure 33. The more detailed picture of the Pentagon 7.

fig:Square

example. The result is shown in Figure 33, and explained below. First note that the n value in D of Figure 32 cancels after punctures by the tail-invariance property (Figure 18), as in the last paragraph of the proof of Lemma 3.5; so does the bottom Φ^{-1} in D , by Fact (2) of Lemma 3.2. These components are not shown in Figure 33.

Working downwards from the top left of the pentagon in Figure 33, the three edge deletions cancel both buckle (β^w) values. The value b value at the top of the diagram D is pulled down across the vertex using a VI relation: this has the same effect as an unzip and an orientation switch on the second stand (as this is oriented downwards). The resulting value $S\alpha u(b)$ cancels by the following reasoning – essentially by definition of unzips and orientations switches – which is illustrated in Figure 34:

Given an arrow 'a' ending on strand 'e', unzipping e produces a sum of two arrows $a_1 + a_2$: one ending on each daughter strand. Reversing the orientation of the first daughter strand gives $-a_1 + a_2$. Contracting the two daughter strands to form a U-shape identifies a_1 and a_2, making $a_1 - a_2$ vanish.

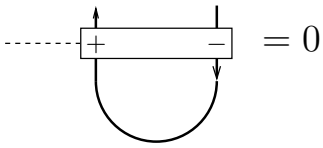

Figure 34. Unzip, switch orientation and connect kills arrows on the strand. fig:KillAn

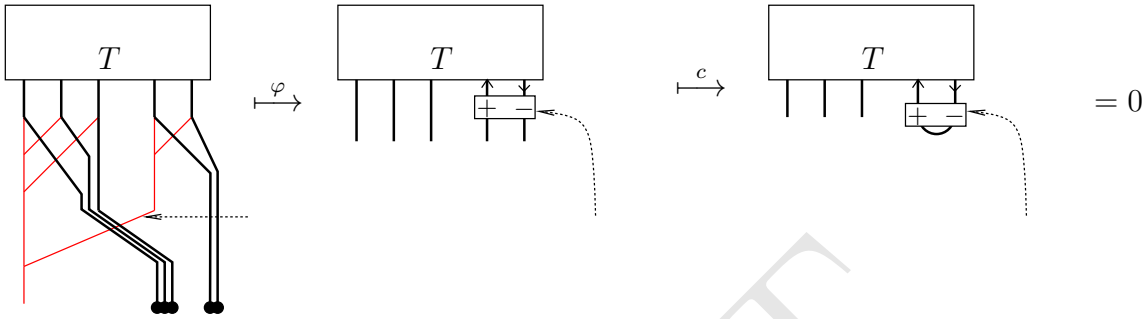

Figure 35. The cancellation of $\varphi(pu(\beta^w))$.

This is exactly what happens to the arrow diagram $S_2\alpha u(b)$ (just under the tangle T in Figure 33) after the edge deletions or contraction, hence this component cancels it in both directions of the pentagon (7). fig:Square7Big

The bottom arrow on the left is the Sorting Isomorphism φ of Lemma 2.4. lem:CapString

On the other hand, working from the top left corner of the pentagon (7) to the right: from Section 3.2, using the strand numbering convention of Figure 15, we have subsec:AEIFormula fig:NumberingK

$$p_1p_3\beta^w = \Phi^{-1}(a_{2(13)}, -a_{2(13)} - a_{4(13)}) \cdot e^{a_{23}/2} \cdot \Phi(a_{23}, a_{43}).$$

This is shown in the enlarged rectangle at the top right corner of Figure 33. The same is true for $pu(\beta^w)$ at the bottom, except with more unzips. fig:Square7Big

From here, the first downward arrow applies the Sorting Isomorphism φ of Lemma 2.4, followed by the contraction and correction term along the second downward arrow. At the bottom of the diagram, $\varphi(pu(\beta^w))$ cancels altogether after contraction, in a similar fashion to Figure 34. Namely, φ and the contraction annihilates any arrow ending on the diagonal red strand, or the double capped strand on the right, as shown in Figure ?? for the diagonal red strand. This cancels each factor of $pu(\beta^w)$. lem:CapString fig:KillAnArrow fig:puBuckle

Of the top $\varphi(p(\beta^w))$ shown in the enlarged rectangle, the Φ^{-1} component cancels by the same contraction argument; only the exponential and the Φ component remains. The arrow in the exponent of $e^{a/2}$ switches sign due to the reversed orientation: this is the $e^{-a/2}$ component at the bottom of the pentagon in Figure 33. After contraction, the Φ component gives rise to a "local" arrow diagram on a single strand shown in Figure 36 and denoted μ. fig:Square7Big fig:mu

In summary, we see that the pentagon (7) commutes if and only if $\mu = \alpha(\nu)$, and otherwise commutes up to a localised error on the contracted strand, of value $\alpha(\nu)^{-1}\mu$.

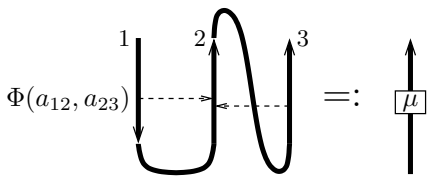

Figure 36. The Φ component of $\varphi(p(\beta^w))$ after contraction. fig:mu

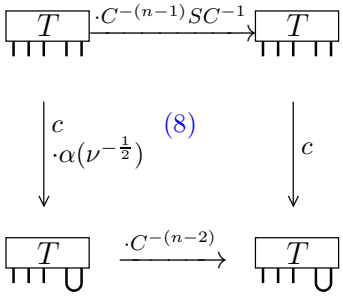

Square (8). Finally, for square (8) we need to check that $C^{-1}S(C^{-1}) = \alpha(\nu^{-1/2})$. Note that the orientation switch negates odd wheels and preserves even wheels, therefore in $C^{-1}S(C^{-1})$ the odd part of C^{-1} cancels, and $C^{-1}S(C^{-1}) = C_0^{-2} = \alpha(\nu^{-1/2})$ by Corollary 3.9. This verifies Square (8). cor:CapValue

We have therefore shown that Z^w commutes with contraction up to an error $\alpha(\nu)^{-1}\mu$ on the contracted strand. It remains to show that this error is 1. This follows from the facts that $Z^w(\uparrow) = 1$, and that Z^w commutes with disjoint unions:

$$1 = c(Z^w(\uparrow\downarrow)) = \alpha(\nu)^{-1}\mu Z^w(c(\uparrow\downarrow)) = \alpha(\nu)^{-1}\mu \cdot Z^w(\frown) = \alpha(\nu)^{-1}\mu.$$

This completes the proof. □

Note that as a side result we have proven the following curious fact about associators:

Proposition 3.14. *For any Φ horizontal chord associator, μ defined from Φ as in Figure 36, and ν the Kontsevich integral of the unknot, $\mu = \alpha(\nu)$.* □ fig:mu

The value V constructed in this section differs, on first glance, from the value V_β constructed in Section 3.1. In the next lemma we show that in fact $V = V^\beta$: this serves both as a reality check, and as a technical tool for showing – in Theorem 3.18 – that Z^w_ξ satisfies the Cap equation. subsec:Part1 thm:ZwExpansion

Lemma 3.15. *The two vertex values from the buckle and the double tree constructions coincide: $V_\beta = V$.*

Proof. In text we denote the positive *sKTG* vertex by $\curlywedge$. Notice that $\wp(\curlywedge)$ – as in Figure **??** – is an *sKTG* which can be built from simpler *sKTG*s by inserting the buckle B^u into $\wp(\uparrow)$ followed by an unzip: see Figure **??**. We computed $\xi(\uparrow)$ in Lemma 3.8. Since Z^u is compatible with insertions and unzips, $Z^u(\curlywedge)$ can be computed by inserting the buckle value β^u (computed in Section 3.2) into $Z^u(\wp(\curlywedge))$. This is followed by applying α and the subsequent cap, unzip and puncture operations. fig:DTofVertex fig:DTofVertex lem:xiofstrand subsec:AEIformula

Because $\beta^w = \alpha(\beta^u)$ is local (is confined to the skeleton of the inserted B^u graph) and in the image of α, all of the cancellations in the computation of $\xi(\uparrow)$ still occur. Hence, $\xi(\curlywedge)$ is as shown in Figure **??**. fig:xiofVertex

To obtain $V = Z^w_\xi(\nearrow\!\!\nwarrow)$, one multiplies $\xi(\curlywedge)$ at each end by C^{-1} or $S(C^{-1})$ depending on orientation, as shown in Figure **??**. Thus, fig:xiofVertex

$$V = C_1^{-1}C_2^{-1}\varphi(p_1p_3\beta^w)u(\alpha\nu^{1/2})u(S(C^{-1}).$$

On the other hand, from Section 3.2, we have:

$$V^{\beta} = C_1^{-1} C_2^{-1} \varphi(p_1 p_3 \beta^w) u(C).$$

Thus, we need to show that:

$$C_1^{-1} C_2^{-1} \varphi(p_1 p_3 \beta^w) u(\alpha \nu^{1/2}) u(S(C^{-1}) = C_1^{-1} C_2^{-1} \varphi(p_1 p_3 \beta^w) u(C).$$

Multiplying with $(\varphi(p_1 p_3 \beta^w)))^{-1} C_1 C_2$ at the bottom and by $u(S(C))$ at the top, this simplifies to:

$$u(\alpha \nu^{1/2}) = u(C) u(S(C)).$$

Since unzips commute with orientation switches, it is sufficient to prove that

$$CS(C) = \alpha(\nu^{1/2}).$$

Recall that in $CS(C)$ all odd wheels cancel, hence $CS(C) = (C_0)^2$, where C_0 denotes the even part of C as in Corollary 3.9, and indeed, by that Corollary, $C_0 = \alpha(\nu^{1/4})$, as needed. □

Corollary 3.16. *The "buckle" amd "double tree" constructions lead to the same result, that is, $Z^w_\xi = Z^w_\beta$.*

Proof. Since any homomorphic expansion Z^w of $\widetilde{wTF}$ is uniquely determined by $\pi(Z^w(\curvearrowright))$, this is immediate from Lemma 3.15. □

Recall that strand unzips in wTT are defined for internal strands of a trivalent tangle, which connect a positive and a negative vertex as "distinguished" edge. With this in mind:

Lemma 3.17. *The map Z^w_ξ commutes with strand unzips in wTT.*

Proof. By construction, Z^w_ξ is defined as a composition of a number of maps. We show that edge unzips commute with every one of these maps, hence with Z^w_ξ:

- $\wp$ involves the tangle ends, which are untouched by internal unzips, hence they commute;
- Z^u commutes with edge unzips as in [WKO2, Section4.6];
- α commutes with edge unzips by definition;
- caps, cap unzips and the isomorphism φ commute with internal unzips (like $\wp$) because they are performed at the tangle ends.

□

The following proposition completes the proof of part Part (3) of the Main Theorem 1.1:

Theorem 3.18. *The map $Z^w_\xi : \widetilde{wTF} \to \mathcal{A}^w$ is the unique homomorphic expansion of $\widetilde{wTF}$, which is compatible with Z^u in the sense of the commutative diagram (2).*

Proof. By Proposition 3.5, Z^w_ξ is compatible with Z^u. By Part (1) (Section 3.1) and Corollary 3.16, $Z^w_\xi = Z^w_\beta$ is uniquely determined by Z^u.

To show that Z^w_ξ is a homomorphic expansion, by Fact 2.5 and Theorem 2.6, one only needs to verify that it satisfies the R4, Unitarity and Cap Equations of Fact 2.5. Of these, $R4$ follows from the fact that Z^w_ξ is a planar algebra map, Theorem 3.13. The Unitarity Equation is simply the statement that Z^w_ξ commutes with strand unzips, and hence it is satisfied by Lemma 3.17.

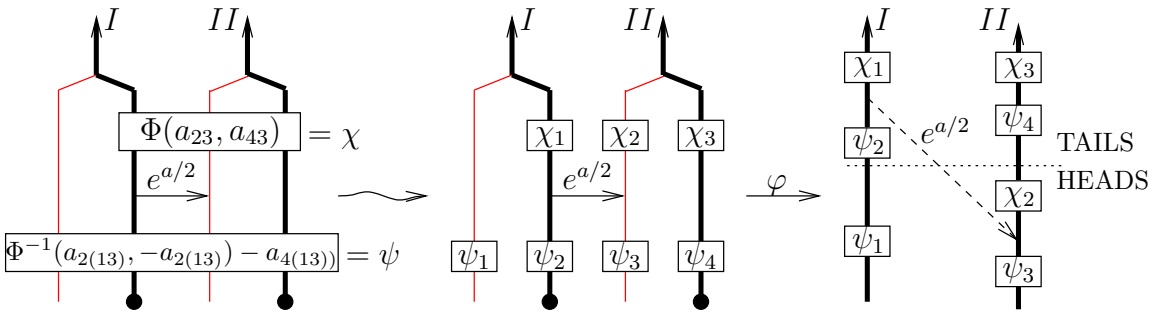

Figure 37. To compute $\varphi(\Phi^{-1}(a_{2(13)}, -a_{2(13)} - a_{4(13)}) \cdot e^{a_{23}/2} \cdot \Phi(a_{23}, a_{43}))$ we switch to a *placement notation* in which we mark on each skeleton strand the elements that have arrows ending on it. For this purpose we denote $\Phi^{-1}(a_{2(13)}, -a_{2(13)} - a_{4(13)}) =: \psi$ and $\Phi(a_{23}, a_{43}) =: \chi$.

fig:ValueV

This leaves the Cap Equation, which we verify directly. By Lemma 3.15 the buckle and double tree constructions yield the same vertex value, therefore it is sufficient to work with the buckle value of the vertex, which was computed in Section 3.1.1. The Cap Equation based on this value, on two bottom-capped stands, reads:

$$u(C)(u(C))^{-1}(\varphi(p_1p_3\beta^w))^{-1}C_1C_2 = C_1C_2.$$

Cancel $u(C)(u(C))^{-1}$ on the left and multiply at the top by $C_1^{-1}C_2^{-1}$, then one only needs to show that $(\varphi(p_1p_3\beta^w))^{-1} = 1$ on capped strands. To show this, multiply on top by $\varphi(p_1p_3\beta^w)$, hence it's enough to see that $1 = \varphi(p_1p_3\beta^w)$. This, in turn, is clear by the CP relation since all heads are below all tails in any value of the isomorphism φ. □

Appendix A. The Alekseev–Enriquez–Torossian formula

app:AET

DON'T BOTHER READING THE APPENDIX. YOU HAVE GIVEN FEEDBACK WHICH I HAVE NOT YET IMPLEMENTED.

This appendix is mainly interesting for readers familiar with the Alekseev–Enriquez–Torossian formula for Kashiwara–Vergne solutions in terms of Drinfel'd associators [AET].

The value $\varphi(\Phi^{-1}(a_{2(13)}, -a_{2(13)} - a_{4(13)}) \cdot e^{a_{23}/2} \cdot \Phi(a_{23}, a_{43}))$ can be computed more explicitly, which is necessary in order to compare it with the [AET] formulas. The first strand of $\mathcal{A}^{sw}(\uparrow_2)$ joins strands 1 and 2 in a vertex, and the second strand of $\mathcal{A}^{w}(\uparrow_2)$ joins strands 3 and 4. Strands 1 and 3 are punctured and strands 2 and 4 are capped. Let us call the two strands of $\mathcal{A}^{w}(\uparrow_2)$ strand I and strand II to avoid confusion. Recall from the construction of φ that one first slides arrow tails from the capped strands "up" through the vertices, then slides all the heads up from the punctured strands 1 and 3. Thus one obtains an element of $\mathcal{A}^{w}(\uparrow_2)$ in which all arrow heads are below all tails on both strands. The result is shown in Figure 37, and explained in the caption.

For a quick re-cap of [AET] notions, let $\mathfrak{lie}_2$ denote the free Lie algebra on two generators x and y. Let $\mathfrak{tder}_2$ denote *tangential derivations* of this Lie algebra, that is, derivations d with the property that $d(x) = [x, a_1]$ and $d(y) = [y, a_2]$, where $a_1, a_2 \in \mathfrak{lie}_2$. Let $\mathrm{TAut}_2 := \exp(\mathfrak{tder}_2)$ denote the group of *tangential automorphisms* of $\mathfrak{lie}_2$. There is a map $\theta : \mathfrak{lie}_2^2 \to \mathfrak{tder}_2$, sending a pair (a_1, a_2) to the derivation d given by $d(x) = [x, a_1], d(y) = [y, a_2]$. The kernel of this map consists only of pairs of the form $(\alpha x, \beta y)$ for α, β constants. In other

words, $\mathfrak{tder}_2$ is "almost" $\mathfrak{lie}_2^2$, and there is a one-sided inverse $\eta : \mathfrak{tder}_2 \to \mathfrak{lie}_2^2$ which sends a tangential derivation to a pair whose first component has no x term and second component has no y term.

A Lie word in x and y can be represented by a binary tree oriented towards a single "head", with leaves labeled by the letters x and y; for details see "primitive elements of $\mathcal{B}_2$" as in [WKO2, Theorem 3.16] and the discussion following it. There is a *tree attaching* map $l : \mathfrak{tder}_2 \to \mathcal{P}^{sw}(\uparrow_2)$, where $\mathcal{P}^{sw}$ denotes the primitive elements of $\mathcal{A}^{sw}$, as follows. Represent the components of $\eta(D)$ by binary trees, and label the heads with x for Lie words coming from a_1, and y for a_2. Then, attach all x-labeled leaves to strand 1, y-labeled leaves to strand 2, and the head below all tails. The order of tails is irrelevant (TC). Conversely, elements of $\mathcal{P}^{sw}(\uparrow_2)$ act as tangential derivations on $\mathfrak{lie}_2$. Wheels act trivially, and thus one obtains a homomorphism $\delta : \mathcal{P}^{tree}(\uparrow_2) \to \mathfrak{tder}_2$, whose only kernel consists only of short arrows on either strand. The map l is a one-sided inverse to δ, that is, $\delta \circ l = \mathrm{Id}_{\mathfrak{tder}_2}$. For more detail see [WKO2, Section 3.2].

Extending δ to exponentials gives a group homomorphism $\delta : \mathcal{A}^w(\uparrow_2)_{exp} \to \mathrm{TAut}_2$, where $\mathcal{A}^w(\uparrow_2)_{exp}$ denotes the group-like part of $\mathcal{A}^{sw}$. For $D \in \mathcal{A}^w(\uparrow_2)_{exp}$, the map δ can be described diagrammatically in the following way. Add an extra (third) strand, and represent a Lie word $v \in \mathfrak{lie}_2$ by a binary tree whose x-labeled tails are attached to the first strand, y-labeled tails to the second strand, and whose head lies on the extra strand. Its conjugate $D^{-1}vD$ is once again a linear combination of such trees (with heads on the third strand), this is the output of the action. See also [WKO2, Proposition 3.19, "Conceptual argument"].

Let V be the Z^w-value of the vertex for a homomorphic expansion Z^w, then $F = \delta(\pi V)$ is a solution to the Kashiwara-Vergne problem in the sense of [AET]. For details see Section 4 of [WKO2]. In particular the [AET] formulas only concern the *tree-level* part $\pi(V)$.

The formula for F presented in [AET, Theorem 4] is[16],

$$F = (\Phi^{-1}(x, -x-y), e^{-(x+y)/2}\Phi(-x-y, y)e^{y/2}), \tag{7}$$ eq:AET

meaning that the automorphism F conjugates x by $\Phi^{-1}(x, -x-y)$, and conjugates y by $e^{-(x+y)/2}\Phi(-x-y, y)e^{y/2}$. This implicitly assumes an "interpretation map" $\Theta : \mathcal{U}(\mathfrak{lie}_2^2)_{exp} \to \mathrm{TAut}_2$. That is, an element $(e^{\lambda_1}, e^{\lambda_2}) \in \mathcal{U}(\mathfrak{lie}_2^2)_{exp}$ is mapped to the automorphism of $\mathfrak{lie}_2$ which sends the generator x of $\mathfrak{lie}_2$ to $e^{-\lambda_1}xe^{\lambda_1}$, and the generator y to $e^{-\lambda_2}ye^{\lambda_2}$. Note that this is not a group homomorphism: composition in TAut_2 is not given by piecewise multiplication of the conjugators.

We relate $\Theta(\Phi^{-1}(x, -x-y), e^{-(x+y)/2}\Phi(-x-y, y)e^{y/2})$ to $\delta(\pi V)$, by constructing a map L which completes a commutative triangle as in Figure 38. At the level of primitives, the map $l \circ \theta$ has the property that $\delta \circ (l \circ \theta) = \theta$. Extend this to the (completed) enveloping algebra $\hat{\mathcal{U}}(\mathfrak{lie}_2^2)$ as follows. An element of $\hat{\mathcal{U}}(\mathfrak{lie}_2^2)$ is an (infinite) linear combination of products of Lie words. As with l, represent each Lie word as a labeled tree, but then attach the products of these labeled trees to the two strands by attaching *all heads* below *all tails*. The order of tails doesn't matter, the order of heads is in the order in which the words were multiplied. Call this map L, and note that L is *not* an algebra homomorphism: it does not respect

[16] There are some notational differences between [AT] and [AET], hence we don't switch strands here as we did in [WKO2]. There are sign differences between the formula (7) and [AET] due to notational misalignment, for example our Φ is [AET]'s Φ^{-1}. Our notation is consistent with all other papers in this series and the formulas are computationally verified in [WKO4].

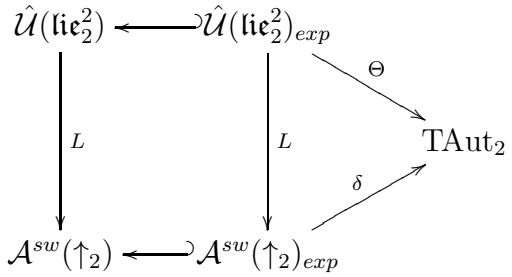

Figure 38. The connection between $\mathcal{A}^{sw}(\uparrow_2)$ and TAut_2. fig:ATInte

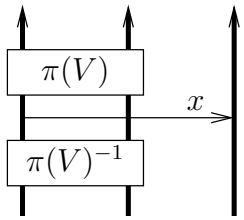

Figure 39. The action of $\pi(V)$ on the generator x of $\mathfrak{lie}_2$. fig:ActOnx

multiplication in $\hat{\mathcal{U}}(\mathfrak{lie}_2^2)$. However, the restriction of L to the group-like part $\hat{\mathcal{U}}(\mathfrak{lie}_2^2)_{exp}$, also denoted L (and which does *not* equal e^l) fits into a commutative triangle $\Theta = \Delta \circ L$.

Now we are ready to compute how $\pi(V) \in \mathcal{A}^w(\uparrow_2)$ acts on the generator x of $\mathfrak{lie}_2$ and match this to the formula (7). Recall the value of $\pi(V)$ shown in Figure 37. The generator x is represented by an arrow from the first strand to the added third strand, and the result of the action is $\pi(V)^{-1}x\pi(V)$, as shown in Figure 39. To compute this, one commutes the tail of x to the top of the strand across $\pi(V)$ using $\overrightarrow{STU}$ relations, thereby $\pi(V)$ and $\pi(V)^{-1}$ cancel, and the result of the action remains. Observe that due to the TC relation, only arrows with heads on strand I act nontrivially on x, in other words only ψ_1 matters, which came from $\Phi^{-1}(a_{2(13)}, -a_{2(13)}-a_{4(13)})$. The arrows a_{23} and a_{43} act trivially on x, so, more simply stated, the action on x is by $\varphi(\Phi^{-1}(a_{21}, -a_{21}-a_{41}))$. Note that $L(\Phi^{-1}(x, -x-y), 0) = \varphi(\Phi^{-1}(a_{21}, -a_{21}-a_{41}))$, so Theorem 1.1 agrees with Formula (7) in the first component.

One can proceed similarly for the second component: the action on y is by

$$\varphi(\Phi^{-1}(a_{23}, -a_{23}-a_{43})e^{a_{23}}\Phi(a_{23}, a_{43})) = L(0, \Phi^{-1}(x, -x-y)e^{x/2}\Phi(x, y)).$$

While this does not match the second component of Formula (7), it only differs from it by a hexagon relation. Alternatively, note that one can obtain the second component of the Formula (7) "on the nose" by starting from an equivalent (isotopic) expression[17] of β^b, as shown in Figure 40.

Some text

References

[AET] A. Alekseev, B. Enriquez, and C. Torossian, *Drinfeld's associators, braid groups and an explicit solution of the Kashiwara-Vergne equations,* Publications Mathématiques de L'IHÉS, **112-1** (2010) 143–189, arXiv:0903.4067.

[17] We thank Karene Chu for this idea.

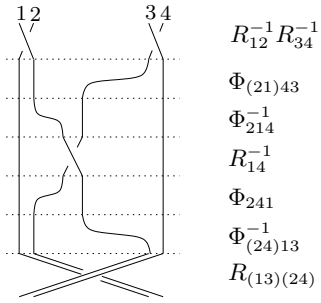

Figure 40. A different expression of β^b.

fig:Buckle

dmanTuraev [AKKN1] A. Alekseev, N. Kazumi, Y. Kuno, F. Naef, *The Goldman-Turaev Lie bialgebra in genus zero and the Kashiwara–Vergne problem,* arXiv:1703.05813.

:GTReverse [AKKN2] A. Alekseev, N. Kazumi, Y. Kuno, F. Naef, *Goldman-Turaev formality implies Kashiwara–Vergne,* Quantum Topology **11-4** (2020) 657–689.

nrenken:KV [AM] A. Alekseev and E. Meinrenken, *On the Kashiwara-Vergne conjecture,* Inventiones Mathematicae, **164** (2006) 615–634, arXiv:0506499.

vNaef:GTKZ [AN] A. Alekseev, F. Naef, *Goldman-Turaev formality from the Knizhnik-Zamolodchikov connection* Comptes Rendus Mathematique **355-11** (2017) 1138–1147

waraVergne [AT] A. Alekseev and C. Torossian, *The Kashiwara-Vergne conjecture and Drinfeld's associators,* Annals of Mathematics **175** (2012) 415–463, arXiv:0802.4300.

-Natan:GT1 [BN1] D. Bar-Natan, *On associators and the Grothendieck-Teichmuller Group I,* in *Selecta Mathematica,* New Series **4**, 183–212, June 1996.

-Natan:NAT [BN2] D. Bar-Natan, *Non-associative tangles,* in *Geometric topology* (proceedings of the Georgia international topology conference), (W. H. Kazez, ed.), 139–183, Amer. Math. Soc. and International Press, Providence, 1997.

Dancso:KTG [BND1] D. Bar-Natan and Z. Dancso, *Homomorphic expansions for knotted trivalent graphs*, Journal of Knot Theory and its Ramifications Vol. **22**, No. 1 (2013) arXiv:1103.1896

BDS:Duflo [BDS] D. Bar-Natan, Z. Dancso and N. Scherich, *Ribbon 2-Knots,* $1+1=2$*, and Duflo's Theorem for Arbitrary Lie Algebras,* Algebraic and Geometric Topology **20** 7 (2020) 3733–3760 arXiv:1811.08558

BDV:OU [BDV] D. Bar-Natan, Z. Dancso and R. van der Veen, *Over then Under Tangles* To appear in the Special Issue in memory of Vaughan Jones, Journal of Knot Theory and its Ramifications. arXiv:2007.09828

lsWheeling [BGRT] D. Bar-Natan, S. Garoufalidis, L. Rozansky and D. P. Thurston, *Wheels, wheeling, and the Kontsevich integral of the unknot,* Israel Journal of Mathematics **119** (2000) 217–237, arXiv:q-alg/9703025.

plications [BLT] D. Bar-Natan, T. Q. T. Le, and D. P. Thurston, *Two applications of elementary knot theory to Lie algebras and Vassiliev invariants,* Geometry and Topology **7-1** (2003) 1–31, arXiv:math.QA/0204311.

o:KIforKTG [Da] Z. Dancso, *On a Kontsevich Integral for Knotted Trivalent Graphs,* Algebraic and Geometric Topology **10** (2010) 1317–1365, arXiv:0811.4615.

HR:CircAlg [DHR1] Z. Dancso, I. Halacheva, M. Robertson *Circuit Algebras are Wheeled Props* Journal of Pure and Applied Algebra **225-12** (2021)

DHR:KVKRV [DHR2] Z. Dancso, I. Halacheva, M. Robertson *A Topological characterisation of the Kashiwara-Vergne Groups* arXiv:2106.02373

HaR:GRTKRV [DHaR] Z. Dancso, T. Hogan, M. Robertson, *A diagrammatic description of the Alekseev-Torossian map,* in preparation.

:QuasiHopf [Dr] V. G. Drinfel'd, *Quasi-Hopf Algebras,* Leningrad Math. J. **1** (1990) 1419–1457.

arAlgebras [J] V. F. R. Jones, *Planar Algebras I* arXiv:math/9909027, to appear in *New Zeland J. Math.*

Conjecture [KV] M. Kashiwara and M. Vergne, *The Campbell-Hausdorff Formula and Invariant Hyperfunctions,* Invent. Math. **47** (1978) 249–272.

:Universal [LM] T. Q. T. Le and J. Murakami, *The universal Vassiliev-Kontsevich invariant for framed oriented links,* Compositio Math. **102** (1996) 41–64, arXiv:hep-th/9401016.

ssuyeau:GT [M] Gwénaël Massuyeau *Formal descriptions of Turaev's loop operations* Quantum Topology **9-1** (2018) 39–117.

urston:KTG [T] D. P. Thurston *The Algebra of Knotted Trivalent Graphs and Turaev's Shadow World* Invariants of Knots and 3-manifolds (Kyoto 2001), Geometry Topology Monographs **4** 337–362, arXiv:math.GT/0311458

Dancso:WKO [WKO0] D. Bar-Natan and Z. Dancso, *Finite Type Invariants of W-Knotted Objects: From Alexander to Kashiwara and Vergne*, paper, videos (wClips) and related files at http://www.math.toronto.edu/~drorbn/papers/WKO/. The arXiv:1309.7155 edition may be older.

ancso:WKO1 [WKO1] D. Bar-Natan and Z. Dancso, *Finite Type Invariants of W-Knotted Objects I: W-Knots and the Alexander Polynomial*, Alg. Geom. Topology **16** (2016) 1063–1133. arXiv:1405.1956

ancso:WKO2 [WKO2] D. Bar-Natan and Z. Dancso, *Finite Type Invariants of W-Knotted objects II: Tangles, Foams and the Kashiwara-Vergne Problem* to appear in Math. Annalen, arXiv:1405.1955

DoubleTree [WKO3] D. Bar-Natan and Z. Dancso, *Finite Type Invariants of w-Knotted Objects III: From Associators to Solutions of the Kashiwara-Vergne problem* (self-reference), paper and related files at http://www.math.toronto.edu/~drorbn/papers/DoubleTree/. The arXiv:????.???? edition may be older.

Natan:WKO4 [WKO4] D. Bar-Natan, *Finite Type Invariants of w-Knotted Objects IV: Some Computations* arXiv:1511.05624

Department of Mathematics, University of Toronto, Toronto Ontario M5S 2E4, Canada
Email address: drorbn@math.toronto.edu
URL: http://www.math.toronto.edu/~drorbn

Mathematical Sciences Institute, Australian National University, John Dedman Bldg 26, Acton ACT 2601, Australia
Email address: zsuzsanna.dancso@anu.edu.au
URL: http://www.math.toronto.edu/zsuzsi